Using Isotopes to Understand the Origin of Water and the Effect of Reinjection in the Los Azufers Geothermal Field in Mexico

by

Ahmad Abuharara

A thesis

presented to the University of Waterloo

in fulfillment of the

thesis requirement for the degree of

Master of Science

in

Earth Sciences

Waterloo, Ontario, Canada, 2017

Author's Declaration

I hereby declare that I am the sole author of this thesis. This is a true copy of the thesis, including any required final revisions, as accepted by my examiners.

I understand that my thesis may be made electronically available to the public.

Abstract

Los Azufers geothermal system is a convective-type geothermal system located northwest of Mexico City in the state of Michoacán at Mexico. Improvements in geochemical techniques enable a better investigation of the Tertiary and Quaternary geothermal reservoir in the Los Azufers field. Traditional stable isotope systems (δ^{18}O, δ^{2}H), nontraditional stable isotope systems (δ^{37}Cl, δ^{81}Br), radioactive isotopes (^{3}H), and radiogenic isotopes (^{87}Sr/^{86}Sr), were utilized to investigate the groundwater geochemistry and detect the circulation of subsurface geothermal water, and consequently determine spatial anomalies in the geothermal activity. Isotopic data indicate recharging of the geothermal reservoir by meteoric water, where, surface water (meteoric water) infiltrated into the deeper sections of the reservoir's formations due to the faulted and fractured structure of the volcanic formations in the Los Azufers field. The stable isotope results showed strong water–rock reactions in the study area, especially in the production zone, indicating the presence of former active fluid circulation systems because of the observed changes in temperature and pressure. Moreover, based on the δ^{18}O and δ^{2}H values, the infiltrating meteoric water mixed with andesitic (volcanic) water produced by water–rock interaction processes. The isotope compositions of the hot springs in the study area indicate direct communication between the surface and the reservoir, and also suggest lateral communication between some reinjection and production wells. The Sr concentrations and isotope ratios (^{87}Sr/^{86}Sr) revealed mixing among waters of different sources, and the extent of water-rock interaction with the different types of igneous rock (rhyolite, basalt, andesite) that formed the reservoirs. The ^{3}H contents suggest a long residence time of deep waters in the reservoir and fingerprint the recharge of water from the surface to the reservoirs. The chlorine (δ^{37}Cl) and bromine (δ^{81}Br) isotopes were used to identify the different sources of waters, but because of the faults it was hard to see correlation in the results. The comparison of the δ^{18}O and δ^{2}H values obtained from the current study with those reported in previous studies suggests that waters are shifting toward andesitic type waters.

Acknowledgement

First and foremost, I thank Allh for his guidance and support. I deem it the utmost honour and privilege to express my innermost gratitude to all individuals and groups that were involved in various ways in carrying out this research work.

I would like to sincerely thank my supervisor, Dr. Orfan Shouakar-Stash, for his unflinching guidance and mentoring throughout this thesis. I would like also to express my genuine appreciation to my co- supervisor, Dr. Brian Kendall his for generous guidance, support and constructive critical insights throughout this thesis.

I would also like to thank my committee members, Sherry Schiff and Daniele Pinti, for their feedback, advice, constructive comments and guidance throughout this study.

My warmest appreciation goes to, Dr. Mustafa Eissa for his supporting and guidance. My gratitude goes to the following who help me on the study field: Nart ,Amjad, Kamal ,Oya ,and Mirana to help me analysis the samples at the laboratory of Isotope Tracer Technologies IT2. A special appreciation goes to Dr. Aida, Sandra, Aurora, and Mary nee at Mexico. I think Laura Groza at the University of Waterloo (Earth and Environmental Sciences department through the Groundwater Geochemistry and Remediation Research Group for chemical analyzes.

I would also like to gratefully acknowledge the support from my teachers Margaret, Elizabeth, Tanya, Kim, David, Liz, Feith, John, Dara, Dr. Christa, and Dr. Stephen at Renison College for learning English.

Thank you to my friends in and out-side Canada. Special thanks to, Osama Ramadan, Mustafa Jaber, Ibrahim Al Futaisi ,Ghaith Bomkhatrh, Rezqallah dance, Siraj Issa, Anas al-Mahmoudi, Mohamed Mokhta,r Belkasem Fathi, Salim Ali, Fathi Al sharif ,Zubair Boucif ,Abdel Sayed Hassi, Dr. Osama Al-Falah ,Dr. Fawzi Abdel Azim, Idris Hafeez , Abdullah Ibrahim ,Kamal Ibrahim ,Rafe Charfad, Rafe Boumalomh, ,Suleiman palace, Ahmed Boucif, Hamid Ajdidh ,Ehab Eshtewi, Rafe Hamad, Munther Hamad, Mohammed Jibril, Hakeem Drissi , The Legend,Hisham Huni, Murad Alamama ,Teen min, Abdel Basset al-Katani, Mohamed pure, Jibril Fetouri, Wael Moneisi and Hossam Alzoubi, Entesar Ashour, Zakia Saaiti, Mohammed Asahvaq, Mohammed Elmokadem, Ahmed Aobeidallah, Salem shamath, Walid Issa, and

Dedication

This work is specially dedicated to the memory of my father and to my mother, loving family, my friends, and my country Libya.

I also dedicate this work to my older sister. Salwa, no matter what I say, I cannot thank you enough for your support, encouragement, and for being my first teacher.

Table of Contents

List of Figures

List of Tables

Chapter 1 Introduction

1.1. Introduction

Geothermal power is a form of power generation derived from the natural heat generated within the Earth's core, mantle, and crust. Heat inside the Earth's crust and mantle is continuously generated by the decay of the long lived radioactive isotopes like uranium, thorium and potassium, and the heat escapes to the Earth's surface through convective and conductive heat transfer processes. Due to these processes, the temperature within the Earth's crust increases with depth. The heat is not spread evenly through the crust and the uppermost mantle because thermal conduction through the lithosphere is low. Plate boundaries are very important areas of volcanic activity and heat loss. Zones of high heat are sometimes located within a few kilometers of the Earth's surface. The challenge is how to exploit such an immense reservoir of abundant energy (Marini, 2000). Geothermal heat can also reach all the way up to the Earth's surface in the form of hot magma or lava; however, in this form the heat is not useful from a technological standpoint. Heat energy is stored by magma in the Earth's crust, and results in the heating of nearby rock and water (magmatic water, metamorphic water, or meteoric water that has seeped deep into the Earth). Some of this heated water travels through faults and cracks in the Earth's crust and reaches the surface; however, most of it is trapped deep underground, and accumulates in cracks and porous rock. This natural accumulation of superheated water beneath the Earth's crust is called a geothermal reservoir. Some geothermal reservoirs, or aquifers, are covered by impermeable rock, which prevents easy access (Taylor, 2007). In such cases, well drilling is required to reach these aquifers and utilize the heat from the hot fluids and steam for power generation purposes (Figure 1.1). Moreover, water enters the reservoirs through wells in a process called re-injection, which helps make up for the liquid extracted during the production of geothermal energy and thus extends the life of the well and the reservoir. Thus, geothermal energy is renewable energy but usually production rates always are bigger than recharge rates (Kagel, 2006).
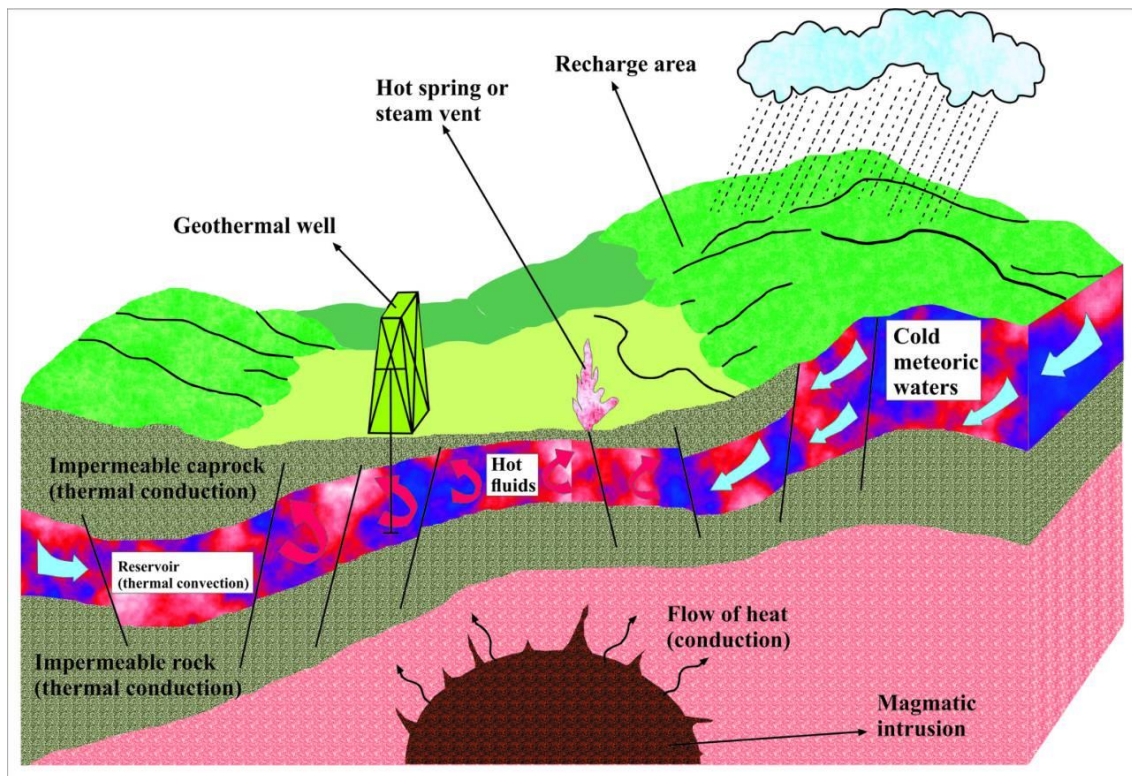
Figure1.1 A geothermal steam field show: recharge area, impermeable cover, the reservoir, and the heat source (modified from Barbier et al., 2002).

1.2. Geological background

1.2.1 Plate tectonics and geothermal fields

Plate tectonic theory, currently accepted by most geologists around the world, accounts for many obviously unrelated geological phenomena. According to this theory, the lithosphere can be divided into separate plates, termed lithospheric plates (Figure 1.2). These plates move slowly across the Earth's surface, typically at a speed of 1-15 cm/year. These plates slide on top of the underlying plastic asthenosphere and pull away from each other (mid-ocean ridges, back-arc basins, and continental rifts), slide past each other (transform faults), or move towards each other (island arc and continental arc subduction zones) (Marini, 2000).

Geothermal fields are areas where the temperature of the groundwater is well above normal values, and this water can be exploited in the production of energy (Barbier et al., 2002). These fields can be found in areas with a normal or slightly above

normal geothermal gradient. Magma located at depths of a few kilometers can cause convective circulation of ground waters, which get heated at depth and subsequently are stored in shallow reservoirs. The most important geothermal areas or fields are located around plate margins. The margins of the plates correspond to weak, densely fractured zones of the crust, and are characterized by intense seismic activity and a large number of volcanoes. Geothermal fields exist in areas such as Hawaii, China, Japan, USA, Italy, Kenya, Turkey, New Zealand, and Mexico (Figure 1.2).
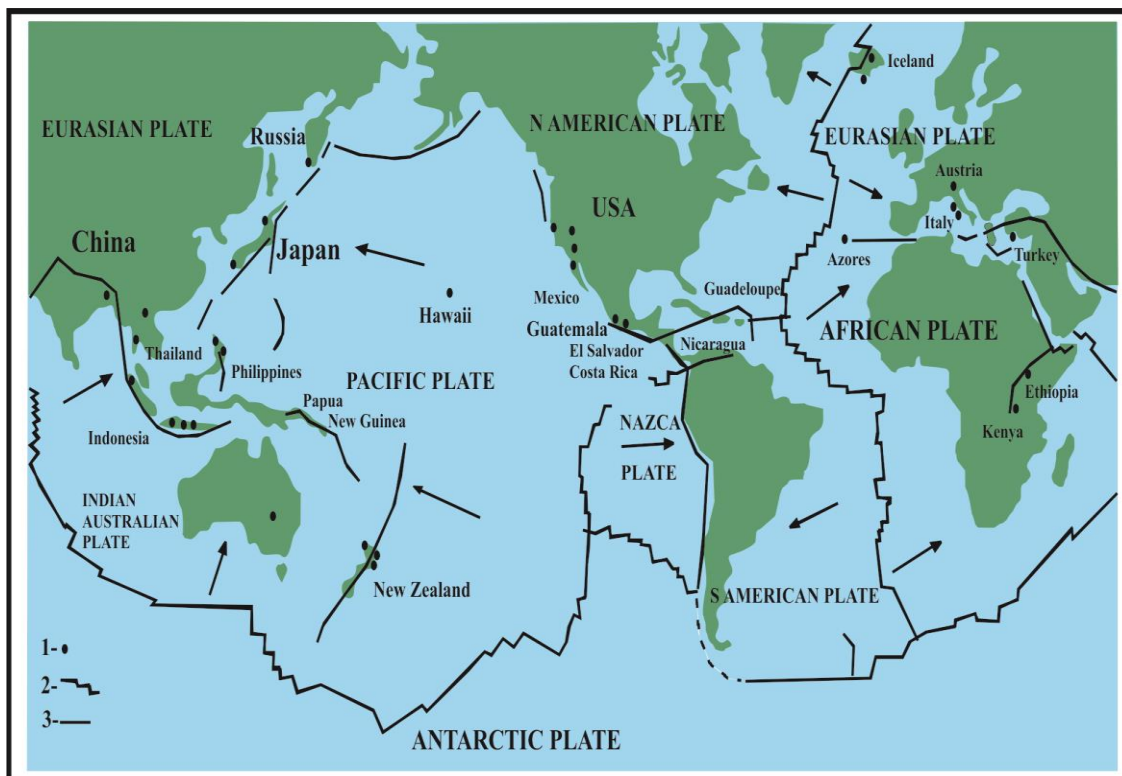
Figure 1.2 World pattern of plates, oceanic ridges, oceanic trenches, subduction zones, and geothermal fields that currently generate electricity. Note: Arrows show the direction of movement of the plates. 1) Geothermal fields under exploitation; 2) Mid-oceanic ridges crossed by transform faults (long transversal fractures); 3) Subduction zones (modified from Marini, 2000).

1.2.2 Generating Electricity: Geothermal Power Plants

A geothermal system is based on the principal of natural convection of fluids. When fluids are confined in a space and heated by an external source, they will transfer heat via convection from the heat source to a colder heat sink (usually the Earth's crust). Geothermal systems consist of three main elements: a heat source, a fluid, and a reservoir, which stores and ultimately transfers the heat (Fridleifsson, 2000). These systems are exploited by geothermal power production plants, which use hot water and

steam from geothermal reservoirs to turn turbine generators, and hence produce electricity. Geothermal power plants do not have to burn fossil fuels to produce steam, and thus they are not a source of anthropogenic carbon dioxide. The main by-product of geothermal power generation is water vapor (Kuo, 2012), and the largest footprint involved with geothermal power generation is in drilling and constructing the well and associated power plant facilities. If geothermal reservoirs are close enough to the surface, this footprint can be minimized; however, well depths can be upwards of two miles deep. To locate reservoirs, geologists use a combination of exploration techniques, including: geological, electrical, magnetic, geochemical, and seismic surveys. If a source is located, exploration wells are then dug to confirm the discovery (Kagel, 2006). Production wells are dug and manufactured later in the process, if the reservoir is to be used for geothermal power production.

The geothermal power generation process proceeds as follows. Production wells, drilled into the geothermal reservoirs build up pressure, which generates a flow of hot steam to the power plant. This hot steam is used to generate electricity in a conventional steam turbine. The steam, after being used to move the turbine, has a significantly reduced enthalpy, and cannot be used again for power generation purposes, and is called waste water and steam. The waste water and steam is re-injected to the reservoir via injection wells where it will be reheated by the geothermal reservoir. This cyclical processing prolongs the life of the well (Barbier et al., 2002) (Figure 1. 3).
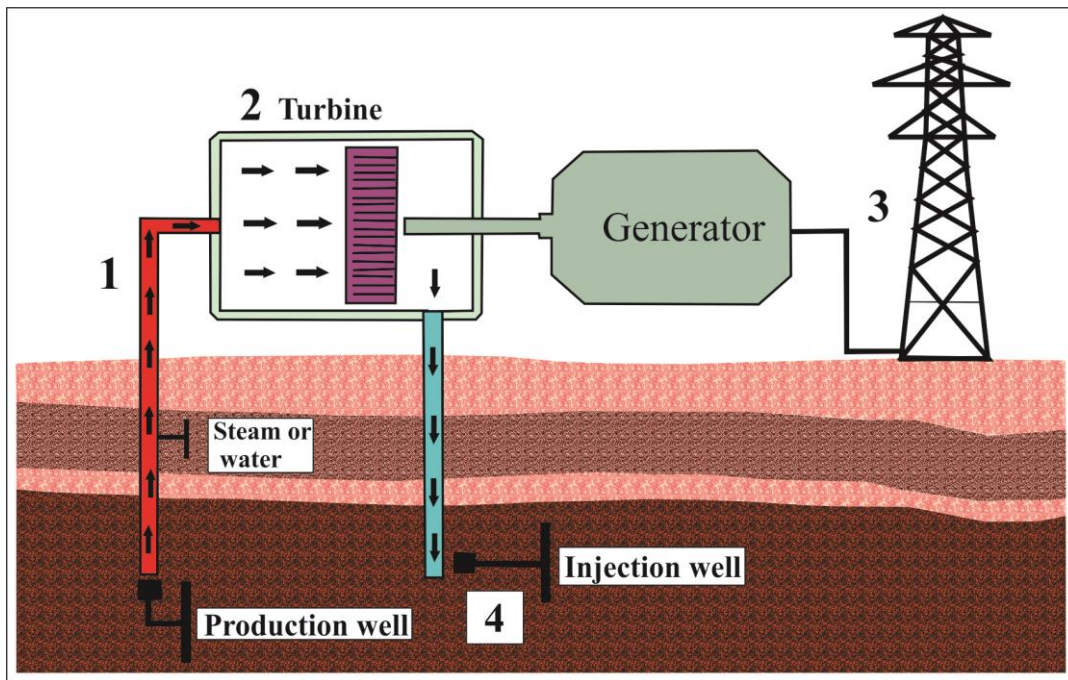
Figure 1.3 Mechanism of the power generation using geothermal energy (modified from http://nothingnerdy.wikispaces.com).

Geothermal fields have been used for power production in the following countries: Chile, Greece, Guatemala, India, Nicaragua, Mexico, and France. Furthermore, many countries are expanding their power production portfolio to include more sustainable production technologies. This is reflected in Table 1.1 (Bertani, 2016), which highlights the geothermal power production facilities currently under construction around the world (Bertani, 2016).

Table 1.1 Global Geothermal Power Plants Under Construction (Bertani, 2016)

Country	Developer	Field	Plant	Year of Operation	PCA (MW)
Ethiopia	Ethiopian Electric Power Corporation	Aluto-Langano			N/A
France	Soultz Geothermal Project	Soultz-sous-Forêts			2
Germany	Enex	Geretsried/Wolfratshausen		2015	5
Germany	N/A	Traunreut		2013	4
Iceland	Reykjavik Energy/ Orkuveita Reykjavikur	Hverahlid		2013	90
Iceland	Alterra Power (HS ORKA)	Reykjanes Expansion	Reykjanes 4	2016	30
Indonesia	PT Pertamina Geothermal Energy	Lumat Balai 1 & 2		2015	110
Indonesia	PT. Geo Dipa Energy	Patuha	Unit 2	2017	110
Italy	Enel Green Power	Bagnore	Bagnore 4	2014	40
Japan	Oita Energy Industry Research Institute	Beppu City		2013	0.003
Japan	GERD, Hirosaki Univ and AIST	Matsunoyu onsen		2012	1
Kenya	KenGen	Olkaria I Unit 4 & 5	Olkaria I Unit 4 & 5	2014	140
Mexico	Mexican Federal Electricty Commission (CFE)	Los Azufres	Los Azufres III	2014	50
Philippines	Energy Development Corp.	Cotabato	Mindanao 3	2017	50
Turkey	Zorlu Enerjii	Denizili-Saraykoy	Kizildere-2	2013	75
United States	Gradient Resources	Patua		2013	60
				TOTAL	767.003

Note: Planned Capacity Addition (PCA)

1.3. Geochemistry Techniques

During the exploratory phase of finding a geothermal reservoir, geochemistry is used to gather detailed information about the potential reservoir. Isotopic techniques can be used to identify the origin(s) of the geothermal fluid. Subsurface temperatures are determined by using chemical and isotope geo-thermometers and mixing models. Fluid flow path in the subsurface can be determined by using tracers and stable isotopes. Furthermore, fluid tracers such as gas concentration mapping (CO_2, Hg) can be used to identify the fluid source, heat source, and fault location (Pang and Ji-Yang, 1990).

Geochemistry can also be used to determine the chemical properties of the fluid and provide data for a conceptual model of the geothermal source that can determine the magma sources of heat and the age of water in the reservoir (Barbier et al., 1983). In general, chemical and isotope geo-thermometers are used to estimate subsurface temperatures of a geothermal reservoir and to monitor temperature changes of the reservoir during production. The most commonly used isotopes in exploration and to determine the geochemical characteristics of aquifers include: hydrogen ($^2H/^1H$ and ^3H), oxygen ($^{18}O/^{16}O$), sulphur ($^{34}S/^{32}S$) and helium (^3He, ^4He) (Pang and Ji-Yang, 1990).

1.4. Background

Mexico is at a decisional crossroads in diversifying its energy sources and the full development (and/or maintenance) of its capacity with regard to geothermal energy. On the one hand, the exploration of new targets has stopped: in recent years, the lack of financial support has limited the development of new geothermal fields such as Las Tres Vírgenes and Los Humeros. Las Tres Vírgenes is the most recent operational field in Mexico. It is located in the center of the peninsula of Baja California. This field has only 4 boreholes and a power plant of limited capacity. Another geothermal field discovered and developed in the early 1980's, Los Humeros, has 24 holes drilled in a Quaternary crater located in the central-eastern part of Mexico, on the eastern edge of the Trans-Mexican Volcanic Belt (in the region of Puebla). This field has recently moved to phase II, almost 30 years after its discovery, and became fully operational with a new power plant of 50 MW commissioned in 2012. New smaller areas, such as Lake Cuitzeo, find themselves only at the very beginning of the exploration phase (see Flores-Armenta, 2012 for a review of the state of the art of Mexican geothermal energy development) and to this day, there have hardly been any extensive studies on these fields.

The other two geothermal fields of global significance in Mexico, Cerro Prieto and Los Azufres, face increasing problems of declining energy capacity and hence reservoir duration. Cerro Prieto is the largest and oldest Mexican geothermal field. It is located in the northern part of Mexico, and its first power units were commissioned in 1973. The commercial operation also began in 1973, so this site has been under extraction conditions for about 40 years. More than 400 geothermal wells have been drilled in 38 years, of which 174 production wells were still operational in 2011. There were also 18 injection wells in operation (Flores-Armenta, 2012). At present, there is an exploration campaign underway and projects are run to regulate the production of steam in order to offset the decline in energy capacity and to achieve a sustainable level of production and power generation.

The decline in energy capacity is related to large-scale extraction in the 1990's, along with the re-injection of cold brine used to maintain reservoir pressure, therefore causing a reduction in the enthalpy of the reservoir. Los Azufres is the second operational geothermal field in Mexico. It has been operational since 1988, with over 100 holes drilled in two separate areas within the crater of Los Azufres. Los Azufres is

a high-enthalpy hydrothermal system associated with a collapsed volcanic caldera, and the reservoir temperature reaches up to 320°C. Los Azufres geothermal energy activities are concentrated in the southern part of the big caldera inside the Morelia–Acambay east–west fault zone in the Trans-Mexican Volcanic Belt (Pasquaré et al., 1988; Ferrari et al., 1991). Several re-injection wells ensure pressure maintenance. However, two separate studies conducted at an interval of 10 years (González-Partida et al., 2005; Pinti et al., 2013) have clearly shown that the invasion of colder water is getting seriously close to the high-enthalpy area of the deposit where the production activities are being concentrated. Although still far from the decreased production of Cerro Prieto, a serious monitoring program has been established at Los Azufres to avoid the reduction of steam production and to allow the development of new production areas.

In order to understand the reservoir conditions in the more recently developed geothermal fields, and their evolution in the oldest fields (Los Azufres), some extensive geochemical studies were carried out in the past (e.g., Truesdell et al., 1979; Welhan et al., 1979; Arnold and González-Partida, 1987; Gonzalez-Partida et al., 1995; Birkle et al., 2001; Verma et al., 2001). However, one of the most powerful markers enabling us to establish the development of geothermal reservoir fluids, namely the isotopes of noble gases, has been largely ignored while exploring the Mexican geothermal fields. Indeed, except for the studies by Mazor and Truesdell (1984), Truesdell et al. (1979), and Welhan et al. (1979) in Cerro Prieto, and some data from Polyak et al. (1985) and Prasolov et al. (1999) in Los Azufres, studies of noble gases are scarce. A few studies deal with the measurements of He and Ar concentrations in several wells at Los Azufres in order to monitor production (Arriaga, 2002; Barragan et al., 2006). Only recently, Pinti et al. (2013) conducted a more extensive investigation of noble gases in geothermal wells and hot springs at Los Azufres as well as carrying out measurements of the stable isotope compositions (^{18}O, ^2H) and radiogenic isotope compositions ($^{87}Sr/^{86}Sr$ ratios). This study allowed, among other things, a better identification of the magma sources of the geothermal field and their geographical extension outside the crater towards Lake Cuitzeo, and showed the increased invasion of the cold brine near the production area. Tritium is a good tracer for the residence time of the waters in the geothermal field and to identify the fresh water input into the system (Ármannsson & Fridriksson, 2009). Stable isotope signatures ($\delta^{18}O$ and δ^2H) can be utilized to

understand the origins of the geothermal waters in the system. Previous studies such as Birkle (2005) and González-Partida et al. (2005) indicated the presence of mixing between meteoric water, andesitic water, and may be some magmatic water in the Los Azufres geothermal system by utilizing stable isotope signatures of $\delta^{18}O$ and δ^2H of the deep geothermal reservoir fluids. Pang et al. (1990 and 1995) stated that δ^2H, $\delta^{18}O$, and tritium contents can be used to trace the origin (meteoric or marine) and the salinity of the water in the reservoir. Moreover, other non-traditional isotopes and radiogenic isotopes are very useful in identifying the origin of groundwater. For example, Sr isotopes are a useful tracer for characterizing the effects of water-rock interaction (Eissa et al., 2016), and Cl and Br isotopes have been used to determine recharge sources and origin for groundwater, and to investigate groundwater mixing (Eissa et al., 2012, 2015, 2016).

1.4.1. The Thesis Objectives

The goal of this project is to evaluate the potential and overexploitation of the geothermal power capacity at the Los Azufres geothermal system in Mexico.

The main objectives of this study can be summarized as follows:

1) Chemical and isotopic characterization of the two parts of the Los Azufres geothermal field (the northern region and the southern region) and identifying similarities and differences between these regions.

2) Identify the main sources of the geothermal waters in the Los Azufres geothermal system.

3) Investigate the effect of the invasion of cold fluid by re-injection in the production areas.

4) Compare the results of this study with the previous results to examine the evolution of the aquifer over the years.

The main tools that were used to carry out this study are chemical analyses of major ions in conjunction with traditional stable isotopes ($\delta^{18}O$, δ^2H), nontraditional stable isotopes ($\delta^{37}Cl$, $\delta^{81}Br$), radiogenic isotopes ($^{87}Sr/^{86}Sr$), and tritium (a radioactive isotope). Utilizing isotopes in this type of study has proved to be successful (Pinti et al., 2013). Gonzales-Partida et al. (1995) have clearly demonstrated that the systematic measurement of stable isotopes in geothermal wells over a period of time is useful in order to determine the evolution of cold water invasion. Comparing the new ($\delta^{18}O$,

δ^2H), (^3H) and isotope and chemical elements data with previous data will be useful for simulating the invasion of cold water into the fields and understand the system.

Chapter 2 : Study Area

2.1. Geological Background of the Study Area

2.1.1. Los Azufres

      Los Azufres is so named because of the presence of small and rare deposits of local sulphur around some of the field's natural geothermal manifestations. The field is located in the state of Michoacán, about 90 km east of Morelia, and about 200 km to the northwest of Mexico City. Los Azufres is the second most essential geothermal field in the country after Cerro Prieto in the north (Figure 2.1). The field is located at 2,800 m above sea level, and is surrounded by a forest of pine trees and valleys (Hiriart and Oct, 2003). In 1975, exploratory studies began in Los Azufres and one year later, the first exploratory well was drilled. The first power units were authorized in 1982, and consisted of five 5-MW back-pressure turbines strategically placed across the geothermal area. The Comisión Federal de Electricidad (CFE) recently authorized new geothermal power plants consisting of four separate 25-MW units, fueled by 14 production wells (Hiriart and Oct, 2003). There are 43 production wells and 6 injection wells producing 14.7 million tonnes of steam and generating 185 MW from 1 condensing unit of 50 MW, 4 condensing units of 25 MW each, and 7 back pressure units of 5 MW each. At this time in the northern part of the geothermal field, there is one 50 MW condensing unit under construction that will replace 4 units of 5 MW each to increase the total electric generation in this field to 215 MW.

2.1.2. Geology

      The geology of the Los Azufres field has been studied by analysis of drill cuttings, geological surface and subsurface mapping, and data from the numerous deep production and injection wells in the field. Collectively this information provides comprehensive geological information on the region. This section gives information about the geologic characteristics of the field such as stratigraphy, structure, and hydrothermal alteration.

Figure 2.1 A map of Mexico with the location of the Los Azufres and Cerro Prieto geothermal fields (modified from Pickler, et al, 2012).

2.1.3. Stratigraphy

The geothermal field in Los Azufres is one of the Pleistocene silicic volcanic zones with geothermal systems in the Trans Mexican Volcanic Belt (TMVB) (Dobson and Mahood, 1985; Verma, 1985; Anguita et al., 2001). Volcanic rocks in the Los Azufres geothermal field have been divided into four main units (Cathelineau et al., 1987; Dobson and Mahood, 1985):

1) The first unit is called Mil Cumbres Andesitic Unit. This unit has a thickness of 2700 m accounting for the entire reservoir rocks that are found in most of the field extending under sea level. The unit consists of pyroclastic rocks and interstratified magma flows of basaltic and andesitic composition, and it forms the local basement in the field. The age of the volcanic rocks ranges between 18 and 1 Ma (Dobson and Mahood, 1985).

2) The second unit is called Agua Fría Rhyolite Unit. This unit has a thickness of 1,000 m. The unit consists of a rhyolite lava. This unit forms the main aquifer with fluid flowing through fractures, and those waters sometimes reach the surface as hydrothermal fluids. This unit can be found at the southern and central part in the field

12

at a shallow level. The age of the volcanic rocks ranges between 1.0 and 0.15 Ma (Dobson and Mahood, 1985).

3) The third unit is called Dacita Tejamaniles. This unit can be found locally in the southern sector of the field, and it comprises young lavas that overlie the Agua Fría Rhyolite (Anguita et al., 2001).

4) The fourth unit is called Tuff (pumice flow deposits). This unit is found near the geothermal field and is associated with young volcanic activity . The unit includes a variety of young, superficial pyroclastic deposits (Cathelineau et al., 1987).

Reservoir rocks in the study area consist of rhyolite, basalt, tuff, and andesite (Figure 2.2).
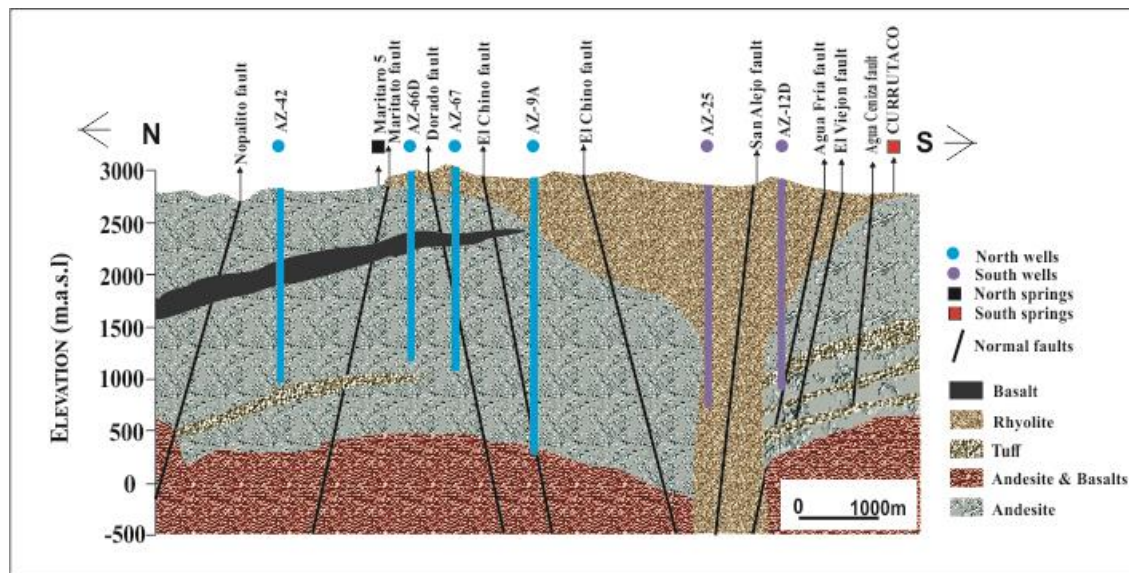
Figure 2.2 A north-south geological cross section of the Los Azufres geothermal field (modified from Arellano et al., 2005).

2.1.4. Structure

In the Los Azufres field, faulting has occurred along three principal directions, namely NW-SE (or NNW-SSE), NE-SW, and E-W arranged from youngest to oldest (De la Cruz et al., 1982). The E-W trend is the most important for geothermal fluid circulation. Geophysical anomalies and geothermal manifestations (such as fumaroles, solfataras, and mudpits) and the significant energy production zones are linked to this fault trend. In the field, most of the fault systems are steeply-dipping normal faults or

inferred normal faults. The names of the faults can be found on the geological map of the area shown in Figure 2.3 (West JEC, 2007; Martínez, 2013). The northern and southern sectors are geologically faulted (Martínez, 2013; West JEC, 2007). The Los Azufres fault system includes the E-W trending Laguna Larga, El Chino, Espinazo del Diablo, Coyotes, and Maritato y La Cumbre faults, and in the south sector are the E-W trending San Alejo, Agua Fría, Puentecillas, Tejamaniles, and Los Azufres y El Chinapo faults. The NE-SW trending faults in the south are El Vampiro, El Viejon, and Agua Ceniza faults and the ones that occur in the north are the Nopalito and Dorado faults. The NNW-SSE trending faults (La Presa, Laguna Verde and Río Agrio) are located in the north zone. These transverse faults could be considered the pathways for the subsurface movement of geothermal fluids, which allow discharge along fault planes, particularly in the southern region of the Los Azufres area. In addition, the presence of these numerous vertical fault swarms may divide the aquifer into customary zones that have diverse regional extent (Figure 2.3).
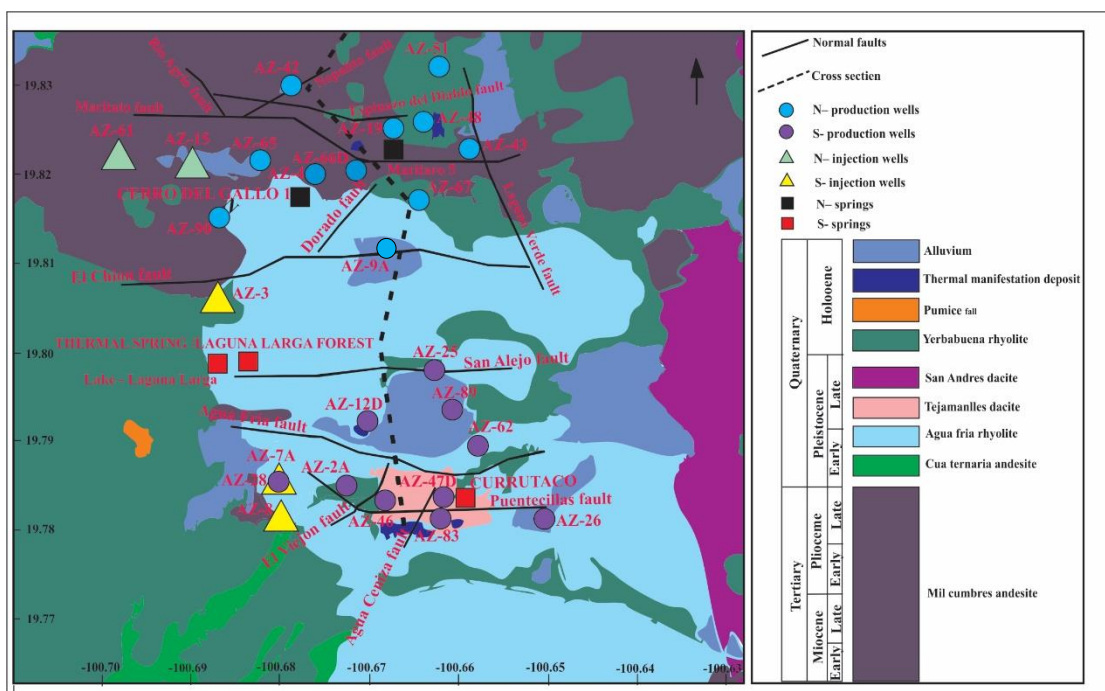
Figure 2.3 Faults, surface geology, wells, and springs located in the Los Azufres geothermal field (modified from Martínez, 2013).

2.1.5. Hydrothermal Alteration

Hydrothermal alteration in the Los Azufres geothermal field is exemplary for a high temperature, volcanic-hosted geothermal system. The drill cuttings have the following secondary minerals: clay minerals, chlorite, calcite, pyrite, hematite, epidote, quartz, hematite and other oxides, and hydrothermal amphibole (Martínez, 2013). Hydrothermal mineral assemblages have been identified in different areas depending on the depth of the first appearance in the well of epidote and hydrothermal amphibole. The first appearance of epidote has been found to correlate with formation temperatures of about 250°C, and the first appearance of amphibole coincides with temperatures near 300°C. The first appearance of epidote occurs in the upper part of the productive reservoir zone, and the first appearance of amphibole occurs in the upper part of the base of the productive reservoir.

2.1.6. Production and Reinjection Wells

In the study area, samples were taken from 21 production wells and 5 reinjection wells, including 11 production wells and 2 reinjection wells from the north part of the study area, and 10 production wells and 3 reinjection wells from the south part of the study area.

Chapter 3 : Methodology

3.1. Field Work

Thirty five groundwater samples were collected during November 9-13 of 2014 from 21 production wells (AZ-2A, AZ-4, AZ9A, AZ-12D, AZ-19, AZ-25, AZ26, AZ-28, AZ-42, AZ-43, AZ-46, AZ-47D, AZ-48, AZ-51, AZ-62, AZ-65, AZ-66D, AZ-67, AZ-83, AZ-89, and AZ-90), 5 reinjection wells (AZ-3, AZ-7A, AZ-8, AZ-15, and AZ-61), and from 9 hot springs (Maritaro 5, Lake - Laguna Larga, Las Adjuntas, Hervideros De Zimirao, Currutaco, Thermal Spring / Laguna Larga Forest, Las Orguideas, Cerro Del Gallo 1, and Manantial Agua Fria Camp CFE) (Figure 2.3; Table 3.1).

Table 3.1 Wells and springs sampled in the study area

Names	Wells and Springs
North production wells	AZ-4, AZ9A, AZ-19, AZ-42, AZ-43, AZ-48, AZ-51, AZ-65, AZ-66D, AZ-67, and AZ-90
South production wells	AZ-2A, AZ-12D, AZ-25, AZ26, AZ-28, AZ-46, AZ-47D, AZ-62, AZ-83, and AZ-89
North injection wells	AZ-3, AZ-7A, and AZ-8
South injection wells	AZ-15, and AZ-61
North hot springs	Maritaro 5, Las Adjuntas, Hervideros De Zimirao, Las Orguideas, and Cerro Del Gallo 1
South hot springs	Lake - Laguna Larga, Currutaco, Thermal Spring / Laguna Larga Forest, and Manantial Agua Fria Camp CFE

Most of the wells in the study area were drilled through andesites, andesitic tuffs, and to a lesser extent through basaltic units, but wells AZ-25 and AZ-26 intersected rhyolites and dacites in the first 400 to 500 m depth (Figure 2.2) (Torres-Alvarado, 1996). Water samples were taken directly from the wells and springs using 1L plastic bottles and 40 mL glass bottles, with three plastic bottles and two glass bottles used per well and per hot spring (Figure 3.1). The high temperature of some wells resulted in an output of steaming water. Water samples from these wells were obtained by using a condenser coil hose to connect the steaming water from the well to the water bottle, and passing through a bucket of ice to decrease the water temperature (Figure 3.1).
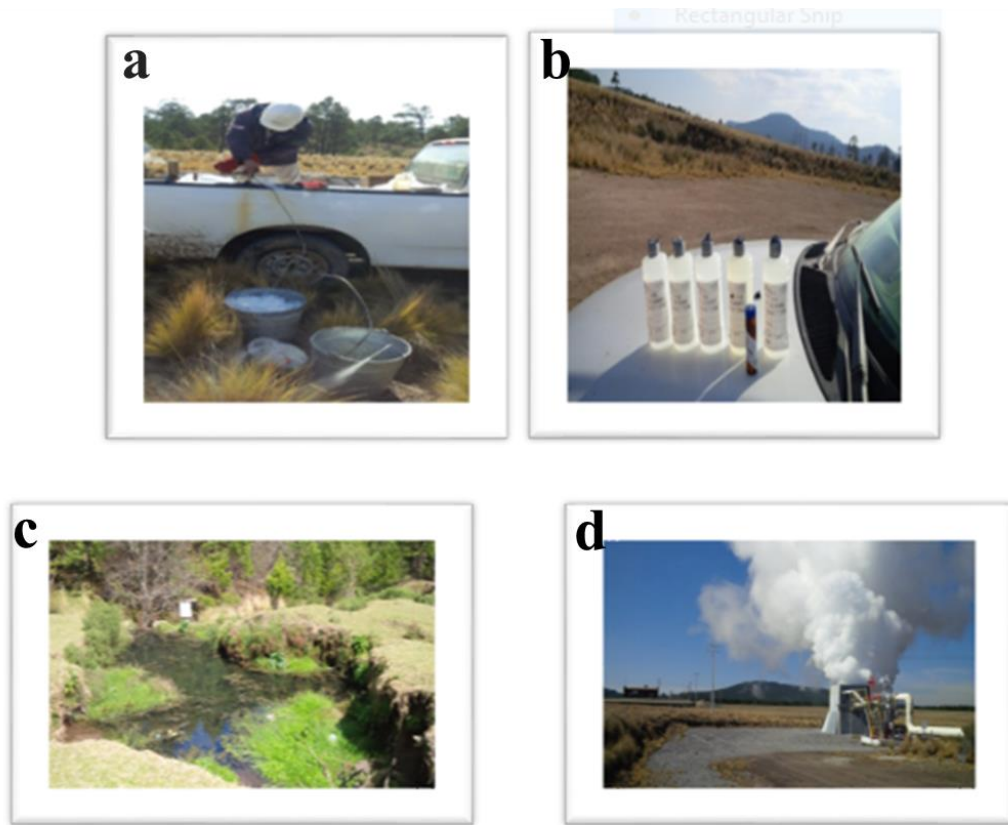
Figure 3.1 Images of water sampling collection locations at the Los Azufres field, (a) well water samples, (c) hot spring, (d) production well. Typical quantity of water collected from each location is shown in (b).

A Global Positioning System (GPS) device was used to identify wells and spring sites when sampling from each well. Various contour maps of the area were drawn. The temperature of the wells and springs were measured by means of a digital thermometer. In some cases, temperature measurement was difficult because of the area where they are located, so temperature data for one well and seven springs was not obtained. The pH of the fluids was measured at the same time as the temperature. Electrical conductivity (EC) was measured in the field using EC meter model No. 1056.

3.2. Laboratory analyses

The salinity was calculated by summing major cations and anions (K^+, Mg^{++}, Ca^{++}, Na^+, SO_4^{--}, Cl^- + 0.5 × HCO_3^-). Major cation and anion concentrations were analyzed at the University of Waterloo Research Center (Ca^{++}, Mg^{++}, Na^+, K^+, HCO_3^-, CO_3^{2-}, Cl^-, SO_4^{--}). The total dissolved solids (TDS) was calculated at the lab by using the following equation:

$$TDS = keEC$$

The TDS is reported in mg/L and the electrical conductivity (EC) is in micro Siemens per liter at 25°C. The correlation factor (ke) varies by 0. 5 and 0.8. EC meters that read as TDS (ppm) usually use a (ke) of 0.5 or 0.8 depending on the meter used.

For the anion analyses, a Dionex DX600 Ion Chromatography method was used (after dilution with Nanopure water) as it is a very good method to measure trace anion concentrations in samples with high concentrations of the nitrate ion (Kern, 1990). By using a micro bore IonPac® AS15 column, an immediate injection method has been produced. This method is suitable to sensitively identify anions at trace levels with the EG40 Eluent Generator. In addition, this method was also used to identify sulfate, chloride, and phosphate (Liu & Kaiser, 1999). The relative standard deviation was 98-100% of samples analyzed by Ion Chromatography.

An Inductively Coupled Plasma Optical Emission Spectrometer (ICP-OES; Thermo Fisher iCAP 6000) and Inductively Coupled Plasma Mass Spectrometer (ICP-MS; Thermo Fisher X-series II) was used for cation analysis, after diluting samples with 2% HNO_3 (Hannan et al, 2012). The relative standard deviation was 95-100% of samples analyzed by ICP (OES, MS).

The standards repeated after every 10 samples and duplicate samples were also included in the run.

Traditional stable isotopes ($\delta^{18}O$, δ^2H), nontraditional stable ($\delta^{37}Cl$, $\delta^{81}Br$), and radiogenic isotopes ($^{87}Sr/^{86}Sr$), as well as tritium (a radioactive isotope) were analyzed at Isotope Tracer Technologies Inc. (IT^2), Waterloo, Ontario, Canada.

Water samples were analyzed for both oxygen and hydrogen isotopes by Cavity Ring Down Spectroscopy (CRDS) (Picarro, Model L1102-i, USA). The Picarro CRDS

isotopic water analyzer provides both $\delta^{18}O$ and δ^2H ratios with high precision in one fast measurement. The instrument is equipped with a high precision autosampler, capable of making consistent small volume injections into the vaporizer. Three to four calibrated internal standards are included at the beginning and end of every run, as well as after every 10 samples. The internal standards have been calibrated to VSMOW, GISP, and SLAP. The results are evaluated and corrected against standards that bracket the samples, and then reported against the international reference material. The analytical precision for analysis is ± 0.1 ‰ for oxygen and ± 0.6 ‰ for hydrogen.

$$\delta^{18}O\ (‰) = ((^{18}O/^{16}O_{sample}\ /\ ^{18}O/^{16}O_{V\text{-}SMOW}) - 1)\ x\ 1000$$

$$\delta^2H\ (‰) = ((^2H/^1H_{sample}\ /\ ^2H/^1H_{V\text{-}SMOW}) - 1)\ x\ 1000$$

Chlorine stable isotope analysis was conducted on methyl chloride (CH_3Cl) gas after converting chloride ions (Cl^-), in solution, to CH_3Cl gas through a multi-step procedure (Shouakar-Stash et al., 2005a). The ratio of the chlorine stable isotopes ($^{37}Cl/^{35}Cl$) was determined by a continuous-flow isotope ratio mass spectrometer. An Thermo Scientific MAT 253 (Thermo Scientific, Germany) was used to measure Cl isotope ratios, after passing the sample through an Agilent 6890 gas chromatograph (GC) equipped with a CTC Analytics autosampler. All results are corrected and reported against the Standard Mean Ocean Chloride (SMOC). A calibrated internal standard is used during every run. The analytical precision for analysis is better than ± 0.2‰.

$$\delta^{37}Cl\ (‰) = ((^{37}Cl/^{35}Cl_{sample}\ /\ ^{37}Cl/^{35}Cl_{SMOC}) - 1)\ x\ 1000$$

Bromine stable isotope analysis was conducted on methyl bromide (CH_3Br) gas after converting bromide ions, in solution, to CH_3Br gas through a multi-step procedure (Shouakar-Stash et al., 2005b). The ratio of the bromine stable isotopes ($^{81}Br/^{79}Br$) was determined by a continuous-flow isotope ratio mass spectrometry. A Thermo Scientific Mat 253 (Thermo Scientific, Germany) was used to measure Br isotope ratios, after passing the sample through an Agilent 6890 gas chromatograph (GC) equipped with a CTC Analytics autosampler. All results are corrected and reported against Standard Mean Ocean Bromide (SMOB). A calibrated internal standard was used during every run. The analytical precision for analysis is better than ± 0.2‰.

$$\delta^{81}Br\ (‰) = ((^{81}Br/^{79}Br_{sample}\ /\ ^{81}Br/^{79}Br_{SMOB}) - 1)\ x\ 1000$$

Strontium isotopic analyses were carried out on a Triton (Thermo Scientific, Germany) Thermal Ionization Mass Spectrometer (TIMS) after samples were prepared via wet chemistry to isolate and purify the Sr ions. Calibrated internal standards are run at the beginning and end of every run. All results are corrected and reported relative to NIST SRM 987. The analytical uncertainty of the method was better that 0.00004.

Tritium isotopic analyses were carried out on a Liquid Scintillation Counter (LSC) (Packard, USA). 250 ml of sample solutions were cleaned, enriched to concentrate the Tritium in the samples and then prepared to be placed in the LSC to be measured in order to determine the tritium levels in the samples. The analytical precision for the analysis is <0.8TU.

Chapter 4 : Results and Discussion

4.1. Chemical analyses (major cations and anions)

The Los Azufres field lies in a complex Plio-Pleistocene succession of basalts, andesites, dacites and rhyolites, where the volcanic rocks unconformably overlie metamorphic and sedimentary rocks of Late Mesozoic to Oligocene age (Gutiérrez & Aumento, 1982; Dobson & Mahood, 1985). The >2700 m thick lava flows and pyroclastic rocks of andesitic to basaltic composition were formed between 18 and 1 Ma and make up the local basement where the geothermal fluids are found in its middle and lower portions (Gutiérrez & Aumento, 1982; Dobson & Mahood, 1985). Andesite is intruded by mafic basaltic sheets (Arellano et al, 2005). The felsic rhyolitic rocks outcrop in the southern portion of Los Azufres.

The subsurface hydrothermal activity can be divided into two types: alkali chloride, which is under the water table (approximately 400 m below ground surface), and acid sulfate, which is closer to the surface. Three main calc-silicate alteration zones have been defined in Los Azufres and can be identified in the field by mineral assemblages (Viggiano-Guerra & Gutiérrez-Negrín, 1995). The first zone is the shallow zeolite zone that is located above 400 m depth and is composed of calcite, anhydrite, pyrite, smectite, chlorite, quartz (chalcedony), and zeolites (heulandite and laumontite). The temperature in this zone is between 25 and 80°C. The epidote zone underlies the first zone and is an important zone because it contains the producing geothermal reservoir. This zone is located between 400 and 2000 m depth, and is composed of epidote, wairakita, chlorite (penninite), quartz, illite/smectite, illite, calcite, pyrite, and prehnite. The temperature in this zone is between 250 and 285°C. The amphibole zone is the deepest zone located below 2,200 m depth, and is characterized by porosity values less than 3%, temperatures up to 285°C, pressure over 170 bars, and the presence of anhydrous minerals. There is no well tapping into this zone as this zone acts as an aquitard, composed mainly of amphibole, epidote, wairakite, biotite, illite, chlorite, garnet, and diopside (Viggiano-Guerra & Gutiérrez-Negrín, 1995). The temperature at the surface of the production wells was between 77°C and 88°C, and the temperature reached in the reinjection wells was 30-32°C (Figure 4.4). The EC values range between 250 and 18,000 µS/cm. The vast majority of wells and springs yielded TDS values

above 130 mg/L, with a maximum of 9000 mg/L (Table 4.1). Only one spring (site Manantial Agua Faia Camp CFE) has a lower TDS value (66 mg/L). The TDS values are likely elevated due to hot water interaction with reservoir rocks. The southern wells exhibited significantly higher TDS values compared with those located in the northern part of the study area, likely due to the more extensive intrusion of water through the faults in the southern part of the study area.

Calcium (Ca^{2+}) can be found in rocks (e.g., limestone) within the minerals calcite, aragonite, dolomite, and gypsum. Calcium is one of the main cations derived from plagioclase in felsic and intermediate igneous rocks, and the main sources of calcium to groundwater from basalts are plagioclase and pyroxene (Pradhan and Pirasteh, 2011). The concentration of calcium in groundwater from the Los Azufres area has a wide range of 167 mg/l (site AZ-46) to 0.123 mg/l (site AZ-26). High calcium concentrations are recorded in groundwater samples in the southern study area (site AZ-46, AZ-47D, AZ-2A, and AZ-83), with a mean value of 57.2 mg/l. The high calcium concentrations are mainly due to water-rock interaction with andesitic and basaltic rocks that are found at the deep part of the study area. The springs that are located in the north part of the study area (site Maritaro 5 and Hervideros De Zimirao) have a mean calcium concentration of 15 mg/l due to water-rock interaction with basaltic sheet intrusions at shallower depths in the northern part of the study area. In general, groundwater water samples from the northern study area contain low calcium concentrations, with a mean value of 13.4 mg/l (Figure 4.1a)

Magnesium (Mg^{2+}) is the main constituent of the dark-colored mafic minerals associated with igneous rocks, and it can also be found in sedimentary rocks, particularly Mg-rich carbonates and dolomites. The magnesium concentration in the groundwater ranges between 20.2 mg/l (site Maritaro 5) and 0.0016 mg/l (site AZ-90). Magnesium concentrations are high in springs that are located in the northern part of the study area (site Maritaro 5, Las Adjuntas, and Las Orguideas) that are in contact with andesitic and basaltic sheets (Figure 4.1b). As magnesium is an important element in the basalt rocks (pyroxenes, amphiboles, micas, and olivine) (Matthess, 1982; Pradhan & Pirasteh, 2011), magnesium concentrations are particularly high in areas connected with the basaltic sheets. The mean value of the northern springs is 7.96 mg/l, and the rest of the groundwater samples located in the northern and southern part of the

study area had low magnesium concentrations, with a mean value of 1.136 mg/l. Therefore, magnesium concentrations are low at the south springs, some of the northern springs, as well as in the north and south ground water samples due to water-rock interaction with relatively Mg-poor andesitic rocks that host much of the reservoir (Figure 2.2 & Figure 4.1b).

Sodium (Na^+) is a major constituent of more evolved igneous rocks, where it can be found in minerals such as plagioclase, nepheline, albite, and sodalite (Clark & Fritz, 1997). Sodium content in the water samples of the study area varies between 3715 mg/l (site AZ-46) and 1.42 mg/l (site AZ-26).

Potassium (K^+) is common in silicate minerals such as K-rich feldspars like orthoclase, clay minerals like illite, and micas like muscovite and biotite, and other potassium silicates (Appelo & Postma, 1993). Similar to sodium, potassium is plentiful in evolved igneous rocks but has much lower concentrations than sodium in groundwater. This is due to the greater resistance of potassium-rich minerals (compared to sodium-rich minerals) during weathering (Pradhan and Pirasteh, 2011). The range of potassium concentrations in the water samples is from 658 mg/l (site AZ-83) to 1.39 mg/l (site AZ-26).

All the samples of the study area have correlated sodium and potassium concentrations with TDS. Both sodium and potassium are highest in the groundwater samples in contact with rhyolitic and andesitic rocks located in the southern part of the study area, where the mean value of both cations combined is 2860.3 mg/l (Figure 4.1c). The groundwater samples from the northern area also have a relatively high concentration of sodium and potassium (mean value of 2132.2 mg/l), whereas the spring samples have low sodium and potassium concentrations (mean value of 119.5 mg/l) because of a greater extent of interaction with mafic rocks than felsic rocks (Figure 4.1c). These observations are mainly attributed to the leaching of felsic rocks in contact with heated groundwater, as felsic rocks are typically richer in sodium and potassium bearing minerals compared with mafic rocks (Clark & Fritz, 1997). Moreover, one north production well (site AZ-42) plotted far off the trend defined by the other samples because the well crosses the Nopalito fault and may be affected by surface water (thus causing a higher concentration of 2339.5 mg/l).

Table 4.1 Chemical and isotopic data for groundwater and hot spring samples collected November 9-13, 2014, in the Los Azufres area. Wells depths and water levels are in meters; chemical data are in meq/L; stable isotope data are in ‰; ^3H levels are in T. U.

Wells & Springs Names	EC	TDS mg/l	Salinity	Well Depth (m)	T °C	pH mg/l	Ca^{++} mg/l	Mg^{++} mg/l	Na$^+$ mg/l	K$^+$ mg/l	Br$^-$ mg/l	HCO$_3^-$ mg/l	SO$_4^-$ mg/l	Cl$^-$ mg/l	δ^{18}O (‰)	δ^{2}H (‰)	δ$^{87/86}$Sr (‰)	^{3}H TU	δ^{81}Br (‰)	δ^{37}Cl (‰)
AZ-2A	15000	9000	9246.3	1300	88	6.8	119.7	0.1	3164	389	0.12	58.6	273	5517.0	1.29	-36.4	0.703758	<0.8	0	0.1
AZ-3	5000	3000	2851.5	2450	32	6.1	7.6	0.2	914.1	221.9	0.06	29.3	30.3	1662.8	0.21	-38.9	0.703824	<0.8	0.6	0.3
AZ-4	10000	6000	6674.9	1950	79	6.4	14.7	0.0	2020	452.9	0.11	24.4	32.3	4142.8	-0.78	-50.1	0.703832	<0.8	0.0	0.5
AZ-7A	10000	6000	6485.0	1750	32	6.7	56.3	0.1	2042	333.8	0.12	24.4	28.5	4012.2	0.88	-39.4	0.708913	1	0.4	0.7
AZ-8	9700	5820	6012.0	2301	32	6.5	62.3	0.2	1835	371.2	0.12	19.5	22.9	3710.7	0.23	-42.1	0.703634	--	0.0	0.3
AZ-9A	9000	5400	5850.9	2591	83	7.3	32.3	0.0	1886	430.3	0.10	151.3	25.7	3400.9	0.87	-37.0	0.703705	0.2	0.2	0.5
AZ-12D	13000	7800	8152.4	1968	78	6.9	16.9	0.1	2652	635.6	0.17	68.3	18.7	4794.9	-1.60	-52.8	0.703882	1.1	0.3	0.5
AZ-15	4000	2400	2146.0	947	32	3.2	6.6	0.9	1727	142.1	0.10	0	93.2	1251.1	-2.22	-46.7	0.703965	0.9	0.2	0.5
AZ-19	9000	5400	5724.8	1666	32	6.4	10.0	0.1	652.1	411.2	0.03	29.3	25.6	2340.6	-1.65	-53.1	0.703789	0.9	0.4	0.5
AZ-25	8000	4800	4907.3	2075	80	7.6	7.8	0.0	1521	348	0.10	122	25.7	2943.8	-2.13	-54.9	0.70387	<0.8	0.1	0.1
AZ-26	250	150	77.4	1241	42	6.8	0.1	0.0	1.4	1.4	0.01	39.0	51.7	3.2	3.02	-22.3	0.703664	<0.8	--	0.4
AZ-28	1000	6000	7155.8	1680	87	6.3	14.5	0.0	2157	481	0.14	19.5	69.8	4423.7	-0.77	-50.7	0.703666	<0.8	0.5	0.1
AZ-42	16000	9600	5945.1	1814	84	6.5	9.9	0.2	1958	381.5	0.09	29.3	33.4	3547.6	5.50	-33.0	0.703847	<0.8	0.4	0.1
AZ-43	7300	4380	4145.8	1519	79	6.10	10.0	0.0	1267	291.7	0.06	78.1	40.9	2497.0	0.74	-42.8	0.704102	<0.8	0.7	0.2
AZ-46	16000	10800	11438.9	918	79	6.7	166.7	0.2	3715	620.1	0.23	78.1	28.6	6869.3	0.78	-38.9	0.703618	<0.8	0.6	0.5
AZ-47D	7800	9600	10346.4	1520	82	6.7	144.5	0.1	3273	634.4	0.16	63.4	22.4	6240.3	0.72	-40.2	0.703622	<0.8	0.4	0.6
AZ-48	6700	4680	5159.1	2693	87	6.5	5.2	0.1	1640	411.9	0.11	19.5	24.1	3067.9	-1.78	-52.8	0.703396	<0.8	0.6	0.5
AZ-51	6500	4020	3855.6	1842	88	7.3	2.9	0.0	1170	288.9	0.05	68.3	19.0	2340.6	-2.36	-56.5	0.703821	<0.8	0.5	0.5
AZ-61	9000	3900	3654.7	2000	30	3.3	10.1	0.7	1098	258.5	0.06	0	71.6	2215.7	-1.41	-46.9	0.703832	1.1	1.1	0.5
AZ-62	7000	5400	5951.1	1550	80	6.9	14.5	0.1	1903	441.4	0.07	87.8	16.5	3531.7	-0.90	-53.3	0.703738	<0.8	0.6	0.7
AZ-65	10000	4200	4272.9	1810	87	7.3	13.1	0.0	1319	265.8	0.06	78.1	70.3	2565.6	-0.36	-45.4	0.703888	<0.8	0.5	0.5
AZ-66 D	11000	6000	7333.8	1773	77	6.6	11.9	0.0	2219	538.1	0.11	39.0	39.5	4505.8	0.61	-38.0	0.703678	<0.8	0.4	0.8
AZ-67	14000	6600	7327.4	1910	85	6.6	211.1	0.1	2313	544.9	0.07	78.1	28.4	4380.8	-0.58	-51.6	0.703739	0.8	0.8	0.8
AZ-83	13000	8400	9092.9	1827	77	6.6	68.2	0.1	2829	657.8	0.14	48.8	26.0	5487.4	1.61	-34.6	0.703656	<0.8	0.5	0.7
AZ-89	8000	7800	8168.6	1876	77	6.6	19.7	0.2	2540	639.4	0.10	48.8	18.8	4926.1	-1.69	-52.7	0.703938	<0.8	0.3	0.7
AZ-90	1400	4800	5272.7	2230	89	7.0	16.4	0.0	1574	344.4	0.07	53.7	39.7	3271.4	-1.09	-51.5	0.70382	<0.8	0.3	0.7
Maritaro 5	220	840	765.2	-		2.2	69.9	20.3	93.6	31.8	0.01	14.6	269.9	272.3	1.46	-37.8	0.704046	4	0.5	0.5
Lake - Laguna Larga	330	132	101.1	-		1.6	3.4	0.6	16.9	15.4	0.01	0	43.9	21.0	-9.60	-68.5	0.704548	0.9	0.5	0.5
LAS ADJUNTAS	3000	198	221.5	-		2.7	13.7	9.4	39.9	13.0	0.01	234.2	26.1	2.3	-10.4	-72.3	0.703962	0.9	--	-1.0
HERVIDEROS DE ZIMIRAO	5000	1800	2069.2	-		2.6	28.7	0.1	686.8	47.5	0.03	117.1	143.6	1103.8	-6.48	-67.3	0.703892	1	--	0.2
CURRUTACO	440	3000	1309.6	-	27	1.9	0.4	0.3	2.2	6.2	0.01	0	1299.5	0.9	1.19	-39.9	0.70441	2.4	0.4	0.4
THERMAL SPRING /LAGUNA LARGA FOREST	280	264	125.0	-		2.2	1.5	0.2	13.84	19.0	0.01	0	72.0	18.4	-8.23	-63.6	0.704352	2.4	--	--
LAS ORGUIDEAS		168	193.8	-		2.3	11.8	8.7	32.8	11.5	0.01	214.7	19.8	1.8	-9.67	-67.5	0.703945	<0.8	--	0.4
CERRO DEL GALLO 1	1800	1080	551.9	-	56	2.4	3.7	1.4	7.0	10.9	0.01	0	527.8	1.1	-3.16	-46.7	0.704155	1.6	--	-1.1
MANANTIAL AGUA FRIA CAMP CFE	110	66	76.6	-		1.9	2.1	0.4	15.0	12.2	0.01	48.8	6.0	16.6	-9.28	-67.6	0.70427	1.6	--	0.2

Note:EC = Electrical Conductivity, TDS = Total Dissolved Solid, T= Temperature, ppm = parts per million (mg/l), -- = no data

Chloride (Cl⁻) is a relatively abundant anion. It is dissolved mainly from the mineral halite (NaCl) found in sedimentary rocks and soils, and is a major chemical constituent of seawater. There is a small amount of chloride in igneous rocks, but larger amounts are found in sedimentary rocks (Pradhan and Pirasteh, 2011). Chloride is found in igneous rocks within feldspars, sodalite, apatite, and meionite (Matthess, 1982). All samples of the study area define a well-correlated linear trend between Cl⁻ and TDS (chloride contents in the water samples vary between 6869.2 mg/l (site AZ-46) and 0.929 mg/l (site Currutaco). The chloride concentration is high in the groundwater samples located in the southern part of the study area, where the mean value of chloride is 4473.7 mg/l. However, the spring samples have low concentrations (mean value of 159.8 mg/l), and the groundwater samples from the northern area have a lower concentration of chloride (mean value of 3387 mg/l) compared to the southern area (Figure 4.1d). Moreover, one north production well plotted far off the liner trend (site AZ-42), with a value of 2339.5 mg/l which can be due to the fact that the well crosses the Nopalito fault and thus was affected by surface water.

Sulfate (SO_4^{2-}) is dissolved from rocks and soils containing sulfate minerals such as gypsum, and from the oxidation of sulfide minerals. Igneous rocks contain relatively little sulfur in the form of sulfate (which can be found in feldspathoid minerals such as hauyne (Appelo & Postma, 1993), but it contain sulfide minerals, including pyrite (iron sulfide), cinnabar (mercury sulfide), galena (lead sulfide), and sphalerite (zinc sulfide). The main sources of sulfate ions are evaporite minerals such as calcium, gypsum and sulfates of magnesium and sodium (Pradhan and Pirasteh, 2011). The range of sulfate concentrations is from 1299.5 mg/l (site Currutaco) to 5.9 mg/l (site Manantial Agua Fria Camp CFE). The sulfate concentrations are low in the study area with a mean value of 35.8 mg/l, except for high concentrations in a spring located in the southern part of the study area (1299.5 mg/l; site Currutaco) and two springs from the northern part of the study area (site Maritaro 5, and Cerro Del Gallo 1, which have values of 2610 mg/l and 528 mg/l, respectively). These three springs may be affected by different sources of waters in the study area such as surface water. There is no significant difference in sulfate concentrations between the northern and southern parts of the study area (Figure 4.1e).

Bicarbonate (HCO_3^-) and carbonate (CO_3^{2-}) anions are formed by the reaction of carbon dioxide with water and carbonate rocks such as limestone and dolostone. Bicarbonate content in the water samples from the study area varies from 234.2 mg/l (site Las Adjuntas) to none detect (site injection wells AZ-15, AZ-61, Lake - Laguna Larga, Currutaco, Thermal Spring / Laguna Larga Forest, and Cerro Del Gallo 1). Groundwater samples from the north and south part of the study area have a moderate concentration of bicarbonate, with a mean value of 52.17 mg/l (Figure 4.1f). However, two production wells (site AZ-25 and AZ-9A) located at the south and north part of the study area have high concentrations of 122 mg/l and 151.3 mg/l respectively. The southern spring samples have low bicarbonate concentrations with a mean value of 8.13 mg/l, but the northern spring samples (site Las Adjuntas, Las Orguideas, and Hervideros De Zimirao) have the highest bicarbonate concentrations with values of 234.2 mg/l, 214.7 mg/l, and 117.1 mg/l, respectively. These springs could be affected by another source of surface water (Figure 4.1f).
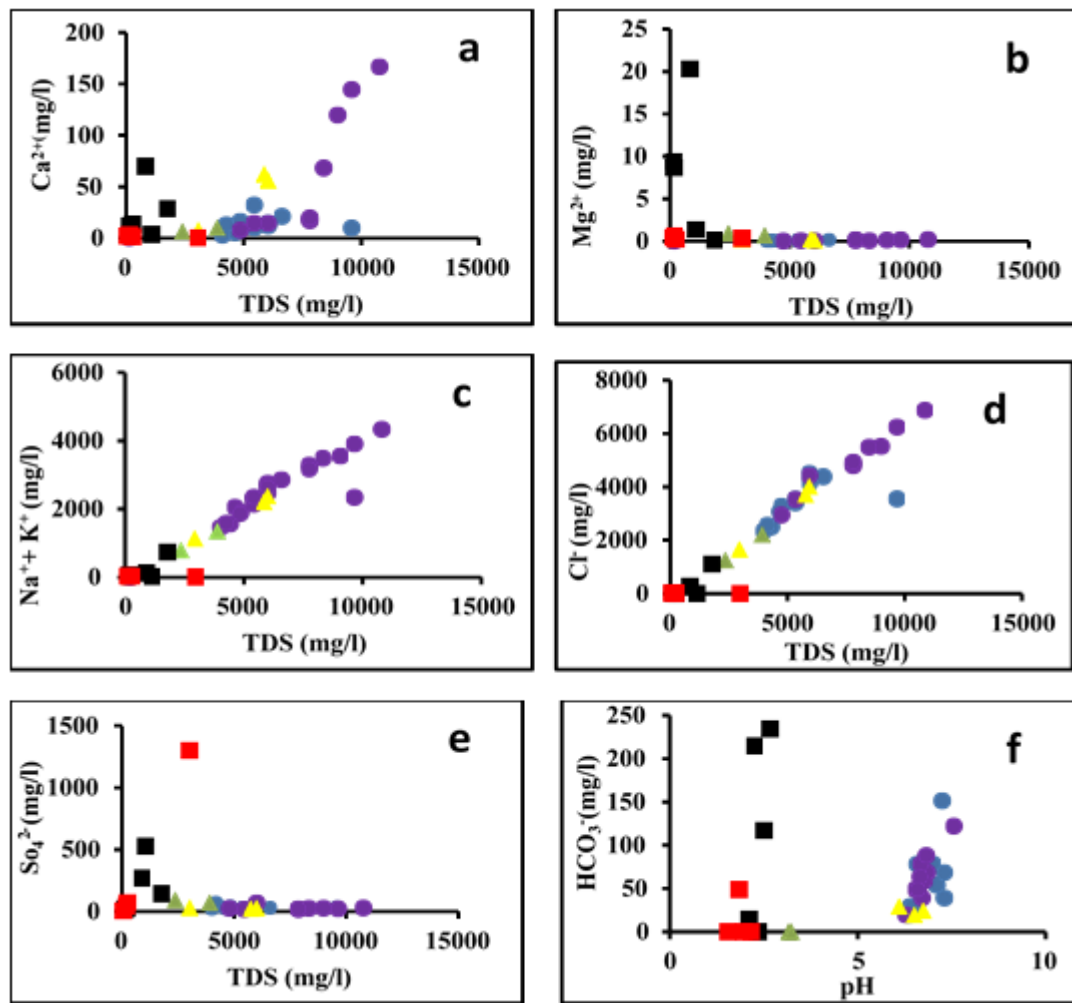
Figure 4.1 Major ion concentrations of injection wells, groundwater wells, and hot springs in the Los Azufres area. TDS = total dissolved solids.

4.2. The water type piper trilinear charts

In this study, the basic chemistry of surface and subsurface water samples in Los Azufres were measured to determine the relative concentration of the cations/anions and water types. Analyses of major cations and anions (Na^+, K^+, Ca^{2+}, Mg^{2+}, HCO_3^-, CO_3^{2-}, Cl^- and SO_4^{2-}) were used to create Piper trilinear charts. The piper trilinear diagram depicts the relative proportions of major ions on a charge equivalent basis for comparison and classification of water samples independent of total analyte concentrations (Hem, 1985). A Piper chart comprises a geometrical mix of two external triangles and a central or inward diamond-shaped quadrilateral based on the relative abundance of different cations or anions (in mg/l). Water types are assigned into zones depending on where these zones fall on the center quadrilateral plot. Every data point is assigned to one water type (Manoj et al., 2013). The major-ion chemistry of groundwater and spring samples (21 production wells, 5 injection wells, and 9 hot springs) from the Los Azufres area can be classified into three groups (Figure 4.2; Table 4.2).

Group I can be classified as calcium-chloride (Ca^{2+} - Cl^-) type water, characterized by an average pH of 2.34 and an average groundwater temperature of around 45°C (Figure 4.2). Group I is represented by two hot springs (Maritaro 5 and Cerro Del Gallo 1) located in the northern part of the study area (Table 4.2).

Group II can be classified as mixed sodium-calcium-bicarbonate (Na^+ - Ca^{2+} - HCO_3^-) type water with a low average pH value (~2.5) and groundwater temperature around 53°C (Figure 4.2). Group II is represented by two hot springs (Las Adjuntas and Las Orguideas), which are located in the northern part of the study area (Table 4.2).

Group III is classified as sodium-chloride (Na^+ - Cl^-) type water with near-neutral pH (6.10-7.58) and a wide range of sampling temperatures (28.0 - 66.4°C) (Figure 4.2). Group III is represented by most samples (21 production wells, 5 injection wells, and 5 hot springs) located in the northern and southern part of the study area (Table 4.2).

Generally, the majority of the deep geothermal waters in the study area have a very narrow range of chemical compositions (high Na^+ contents) due to water-rock

interaction with the andesitic rocks that formed the reservoirs. However, spring waters show a wider range of chemical composition. Spring waters in the north are generally trend toward higher Ca^{2+} and Mg^{2+} contents compared to deep waters, which is probably due to water-rock interaction with basaltic sheet intrusions at shallower depths in the southern part of the study area. Furthermore, spring samples from the northern part of the study show higher diversity of chemical compositions compare to the spring waters from the southern parts of the study area (Figure 4.2). Two of the northern springs show the highest Ca^{2+} and Mg^{2+} contents compared to all other samples from the study area which is probably due to the felsic rhyolitic rocks outcrop in the southern portion of the study area. Similarly, deep geothermal waters show higher Cl^- contents compared to the spring waters, which are higher in carbonate + bicarbonate content as well as sulfate in some cases. The pH for the south production, injection wells, and north production wells is near-neutral (6.10-7.58), but the north injection wells have low pH (3.00 to 3.20) due to reinjection water processing (Figure 4.3).
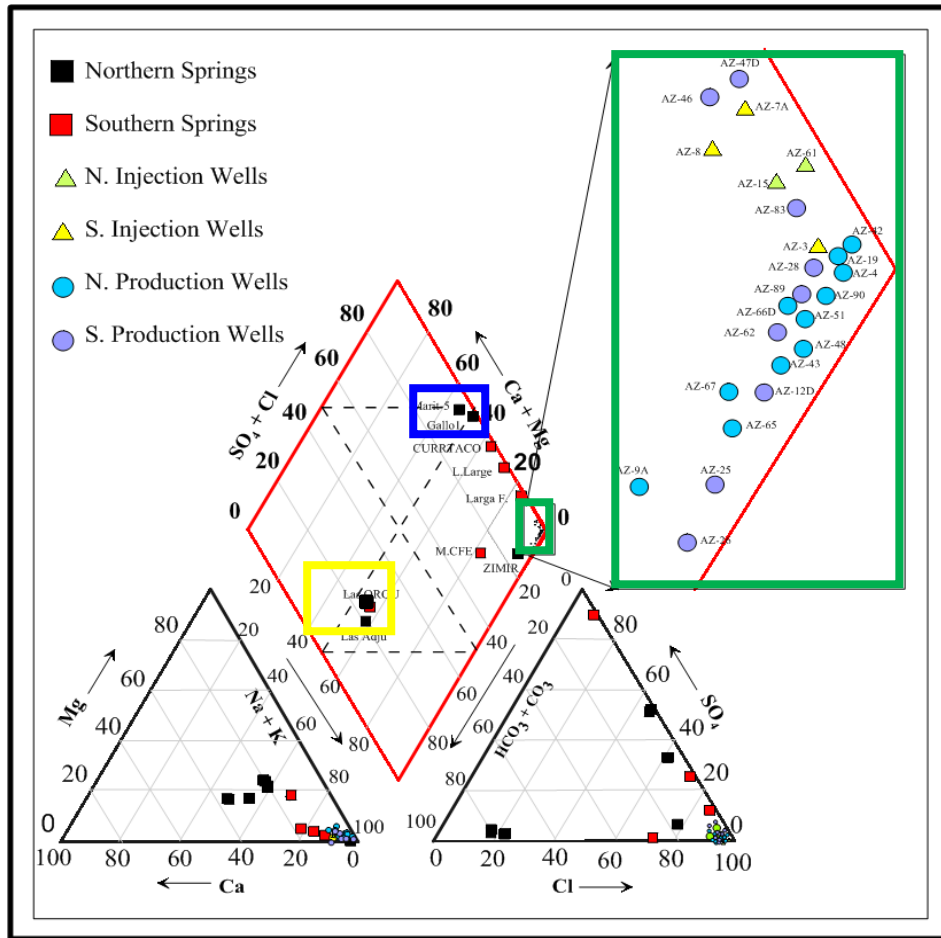
Figure 4.2 Piper Diagram of injection wells, groundwater wells, and hot springs in the Los Azufres Area. ■ **Group 1 (Ca^{2+} - Cl$^-$),** ■ **Group 2 (Na$^+$ - Ca^{2+} - HCO$_3^-$), and** ■ **Group 3 (Na$^+$ - Cl$^-$).**
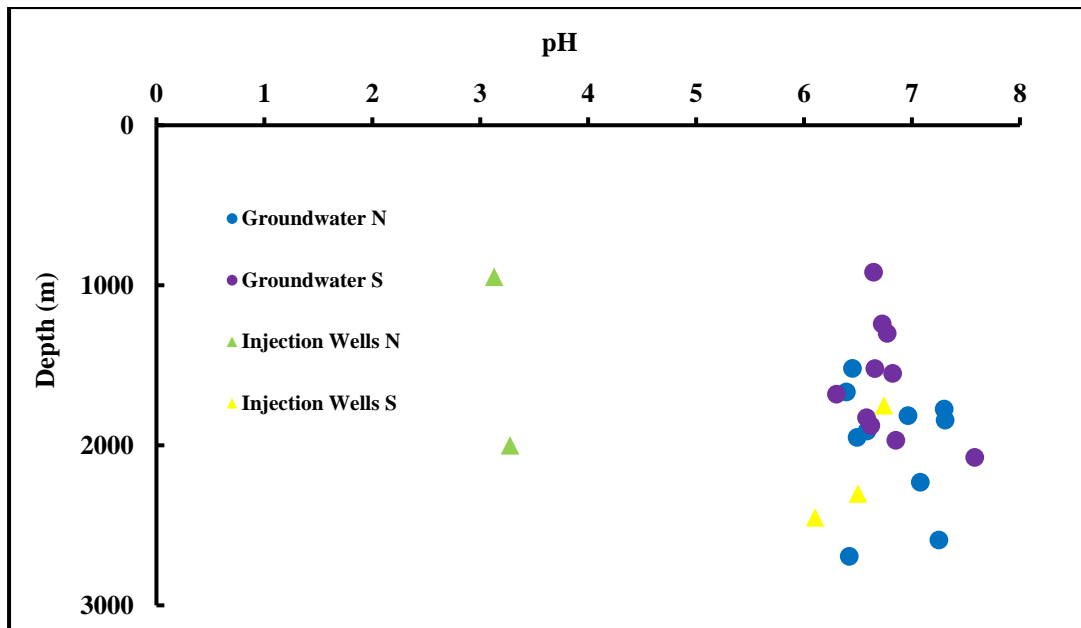
Figure 4.3 pH vs depth (m) of production and injection wells in the study area.
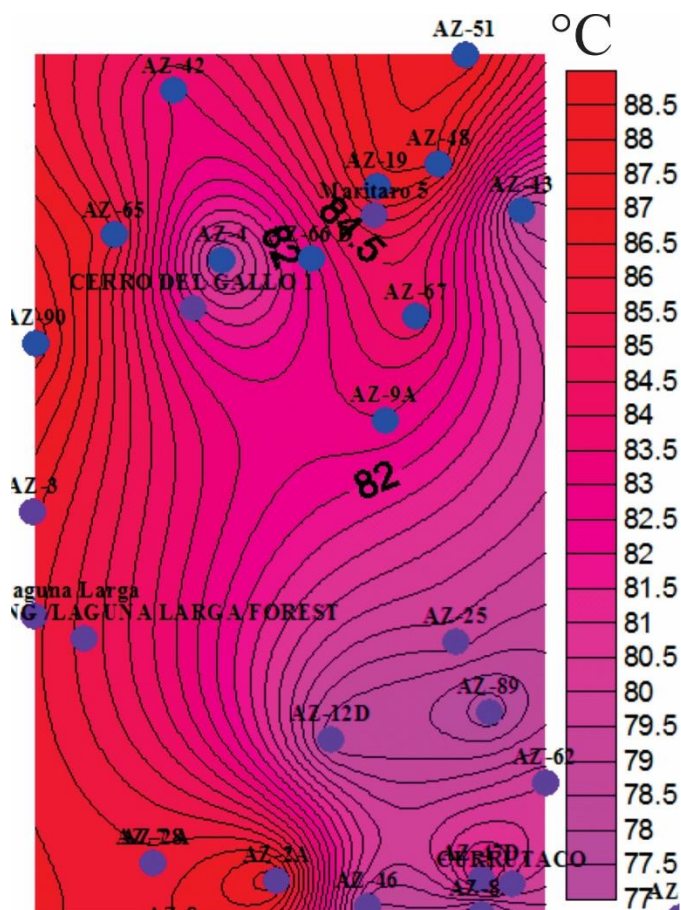
Figure 4.4 Contour map of the groundwater temperature (●north production wells and ●south production wells in the study area (Los Azufres geothermal field).

Figure 4.5 Contour map of the groundwater temperature (⬤north production wells, ⬤south production wells, △ north injection wells, and △ south injection wells) and shallow water temperatures (■north hot springs, ■south hot springs) in the study area (Los Azufres geothermal field).

Table 4.2 Water types in the study area

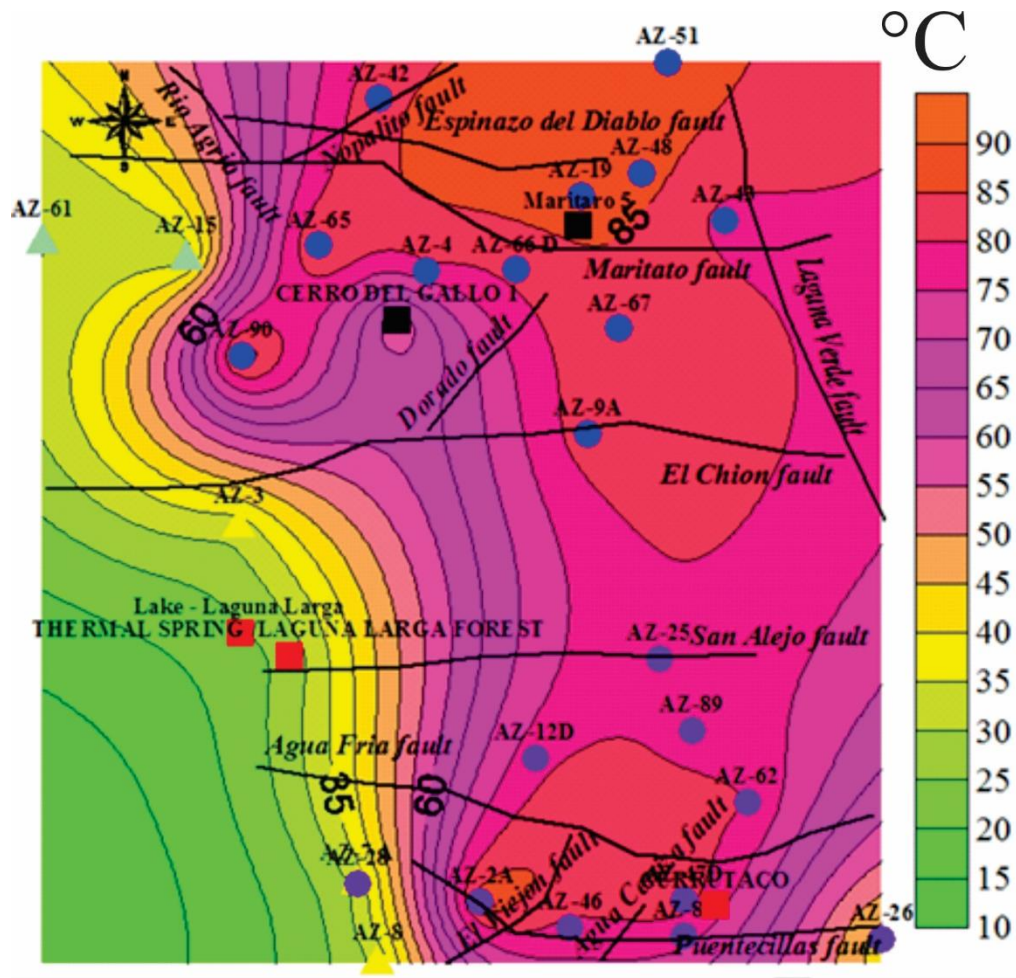| Group I	2 north hot springs (Maritaro 5 and Cerro Del Gallo 1)
Group II	1 north and 1 south hot spring (Las Adjuntas and Las Orguideas)
Group III	21 north and south production wells (AZ-2A, AZ-4, AZ9A, AZ-12D, AZ-19, AZ-25, AZ26, AZ-28, AZ-42, AZ-43, AZ-6, AZ-47D, AZ-48, AZ-51, AZ-62, AZ-65, AZ-66D, AZ-67, AZ-83, AZ-89, and AZ-90), 5 north and south injection wells (AZ-3, AZ-7A, AZ-8, AZ-15, and AZ-61), and 5 north and south hot springs (Lake - Laguna Larga, Hervideros De Zimirao, Currutaco, Thermal Spring / Laguna Larga Forest, and Manantial Agua Fria Camp CFE)

4.3. Isotopes

4.3.1 Oxygen (δ^{18}O) and Deuterium (δ^{2}H)

Isotope techniques can be used to distinguish between origins and different processes that may lead to alteration and the evolution of groundwater, including water-rock interaction and mixing of waters of different composition. In the Los Azufres area, it is necessary to understand the sources of fluids in the geothermal system as well as the groundwater flow system and the movement of re-injected water in the geothermal system. δ^{18}O and δ^{2}H are considered to be ideal tracers that can be used to determine the recharge and mixing source(s) since they are part of the water molecule and are sensitive to chemical and physical processes such as groundwater mixing and evaporation (Dansgaard, 1964; Clark and Fritz, 1997). Therefore, during this study, δ^{18}O and δ^{2}H were used to understand the groundwater circulation in and around the complex hydrothermal system. González-Partida et al. (2005) and Ignacio et al. (2012) utilized isotopes to identify the origin, water-rock interaction, and mixing of waters of different composition.

Groundwater near Los Azufres is comprised of two distinct systems: a shallow, cold water system and a deep, high-temperature hydrothermal system. The isotopic composition of groundwater ranges from +5.50‰ to -10.45‰ for δ^{18}O and from -22.34‰ to -72.26‰ for δ^{2}H (Figure 4.6; Table 4.1). The lightest isotopic signatures for δ^{2}H and δ^{18}O were recorded in spring water at site Las Adjuntas located in the northern

part of the study area, whereas the most isotopically heavy groundwater was recorded in the production well at site AZ-42 located in the northern part of the study area.
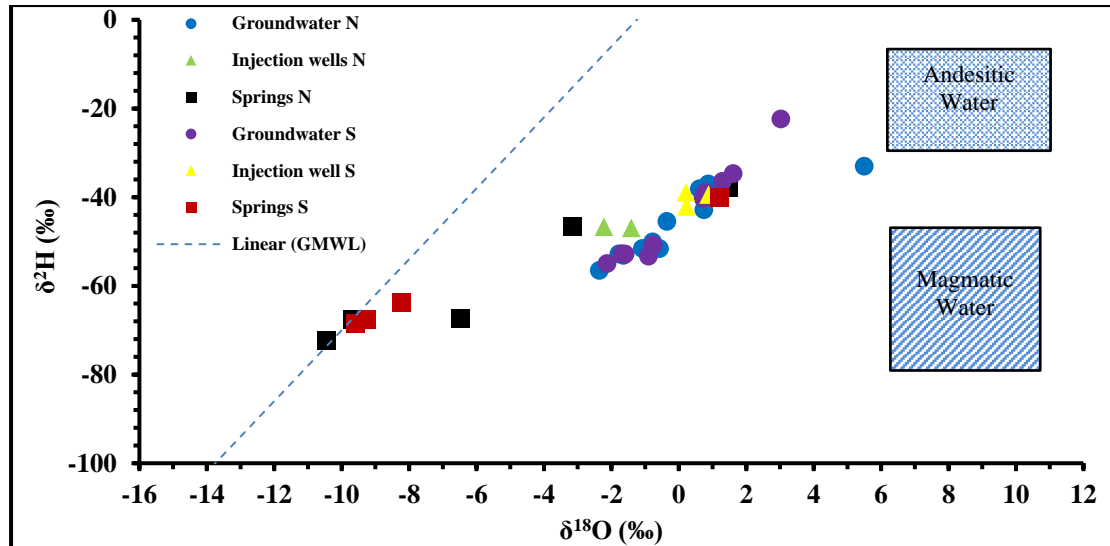
Figure 4.6 $\delta^{18}O$ vs. δ^2H of injection wells, groundwater wells, and hot springs in the Los Azufres geothermal field compared to andesitic water came from water rock interaction with the andesite rock that formed the reservoir rocks and magmatic water released as hydrothermal fluids of magmatic crystallization.

The isotopic signatures of the springs range from -9.28‰ to -10.45‰ for $\delta^{18}O$ and from -67.46‰ to -72.26‰ for δ^2H. Some samples plot close to the global meteoric water line (Gat et al., 1969), but are isotopically depleted relative to local meteoric precipitation (Birkle et al., 2001) and have lower chloride and salinity (Figure 4.8, 4.9). Some springs (Maritaro 5, Cerro Del Gallo 1, Hervideros De Zimirao, Currutaco, and Thermal Spring / Laguna Larga Forest) have higher δ^2H (-37.82‰ to -67.34‰) and $\delta^{18}O$ (1.46‰ to -8.34‰) values, and have much higher chloride and salinity, likely resulting from water-rock interaction and isotopic exchange with feldspars and other silicate minerals in the aquifer (Cole and Ohmoto, 1986) (Figure 4.8, 4.9).
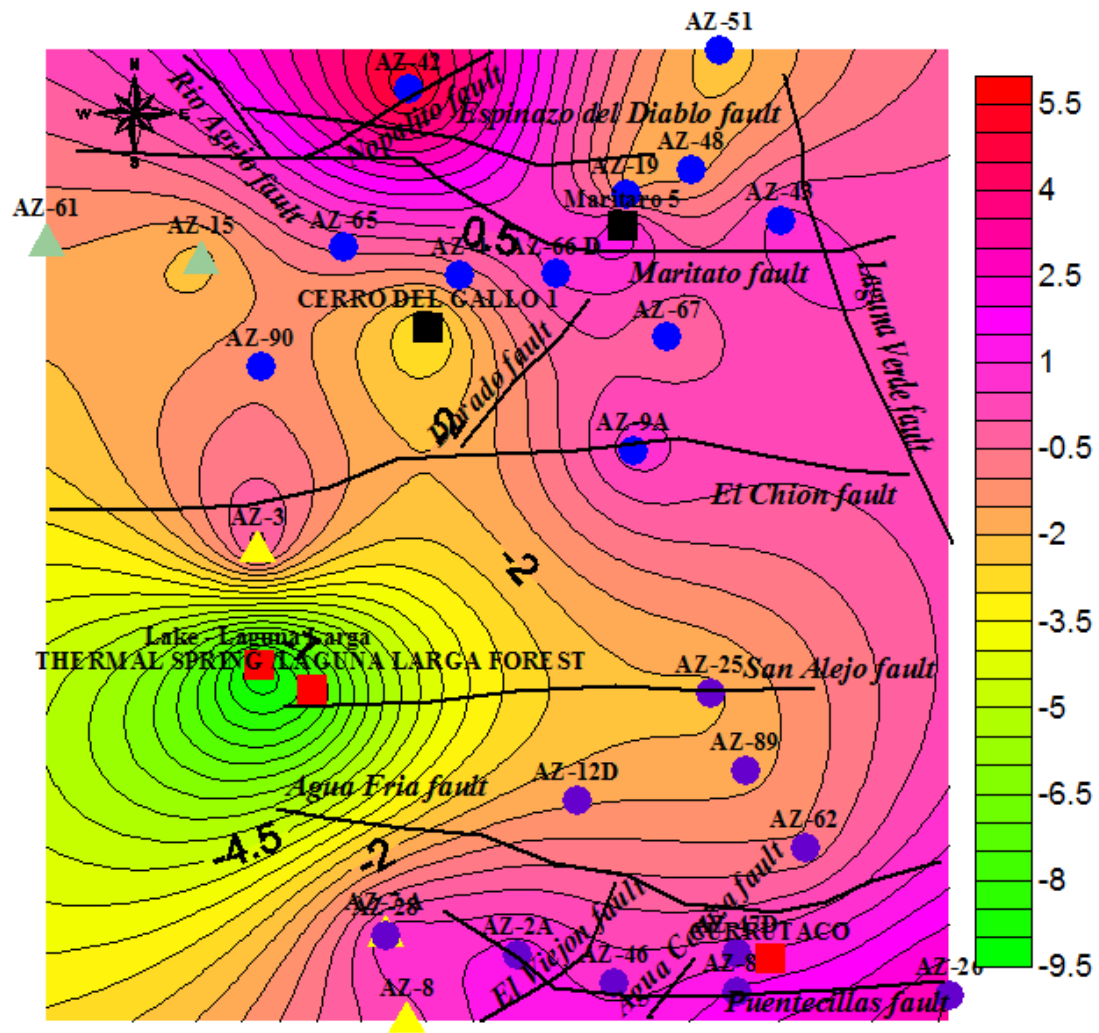
Figure 4.7 Contour map of the $\delta^{18}O$ of groundwater (⬤north production wells, ⬤ south production wells,△ north injection wells, and △south injection wells) and shallow water (■north hot springs, ■south hot springs) in the study area (Los Azufres geothermal field).

The isotopic signature of the production and injection wells located in both the southern and northern Los Azufres areas are moderately enriched compared with the meteoric recharge water that comes from local precipitation. The isotopic signatures of the production wells range from +5.50‰ to -2.36‰ and from -22.34‰ to –56.48‰ for $\delta^{18}O$ and δ^2H, respectively (Figure 4.6). The data from these wells plot between two end members: the recharge meteoric water, and the isotopic signature of andesitic host rocks forming the geothermal reservoir in the study area (Torres & Birkle, 2001). The andesitic volcanism likely originates from the subduction of oceanic lithosphere below the North American Plate during Cretaceous to recent times (Birkle et al., 2001). The northern and southern production wells in the study area fall on the mixing line between

local meteoric water and andesitic water (Figure 4.6 and Figure 4.7). The estimated mixing ratio shows that the production wells are formed by a mixture of local meteoric water and about 55-95% andesitic water (Birkle et al. 2001).
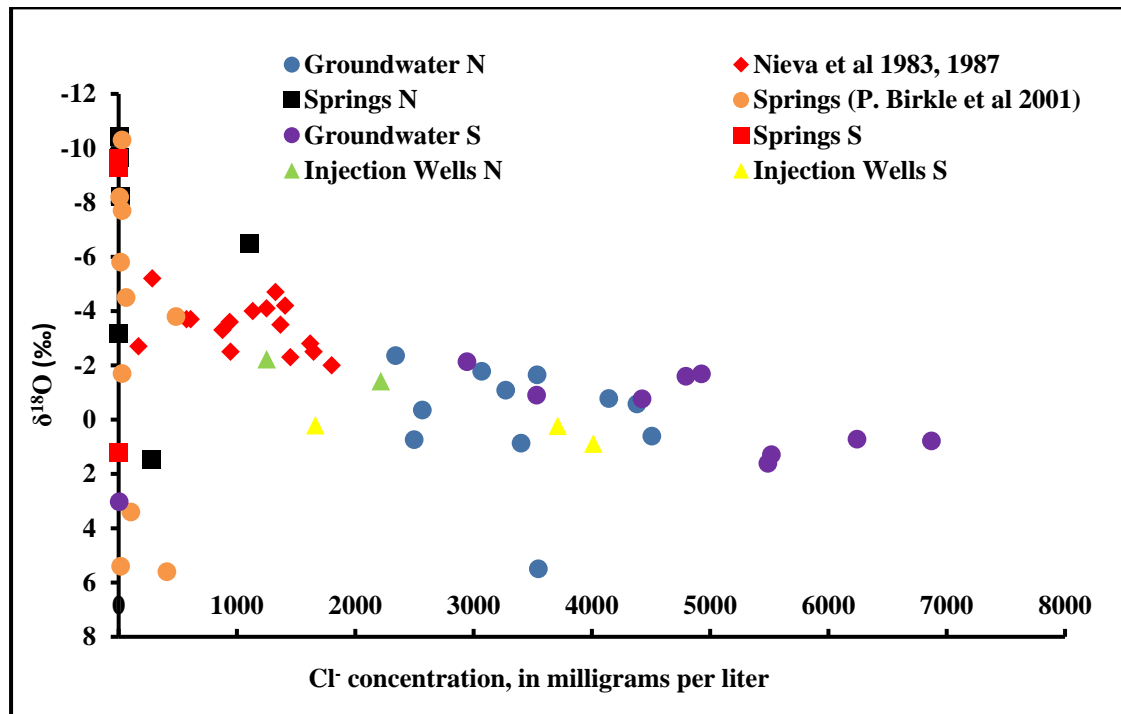
Figure 4.8 δ^{18}O vs. Cl$^-$ concentration of injection wells, groundwater wells, and hot springs in the Los Azufres geothermal field.

The isotopic enrichments characterizing the production wells located in the southern and northern Los Azufres area are mainly due to the water-rock interaction processes occurring at relatively high temperatures close to the boiling point of the fluids deep in the aquifer (González et al., 2005). Geothermal waters showed a positive shift of δ^{18}O from the meteoric water line due to oxygen isotope exchange between the fluid and reservoir materials at different temperatures (Craig, 1963; Truesdell & Hulston, 1980) and/or mixing between meteoric water and deep andesitic water. In addition, the re-injection of groundwater and its circulation deep into the high-temperature hydrothermal reservoir further promotes isotopic enrichments through isotopic exchange and evaporation, and consequently shifts the groundwater isotopic signatures closer to the andesitic water end-member.
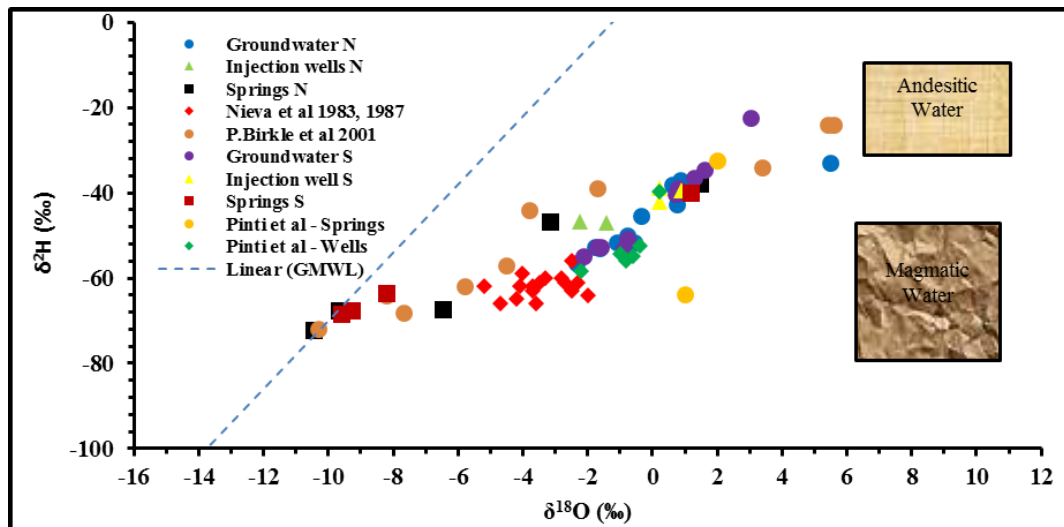
35

Figure 4.9 $\delta^{18}O$ vs. δ^2H of injection wells, groundwater wells, and hot springs in the Los Azufres geothermal field, including data from previous studies (Nieva et al., 1983, 1987; Brik et al., 2001; Pinti et al., 2013). GMWL = Global Meteoric Water Line.

Isotopic exchange in the geothermal system will slowly move the system toward equilibrium, with the isotope exchange rate being faster at higher temperature portions of the system (Clark and Fritz, 1997). In Figure 4.9, a compilation of oxygen isotopic signatures shows a trend of successively higher enrichments from 1983 to 2014 (Nieva et al., 1983, 1987; Brik et al., 2001; Pinti et al., 2013), which indicates high circulation and isotopic exchange processes involving reinjected water. Also, Figure 4.8 shows that the groundwater samples from the south part of the study area have higher Cl⁻ than the groundwater samples from the north part of the study area due to water-rock interaction. Compering the data from the study area with data from previous studies (Nieva et al, 1983, 1987, Brik et al, 2001), the Cl⁻ concentrations have increased over time as a result of water-rock interaction processes, especially at the south part of the study area data, consistent with the observed trend towards higher $\delta^{18}O$ (Figure 4.8).

4.3.2 Strontium Isotopes (^{87}Sr/^{86}Sr)

Strontium (Sr) has four natural stable isotopes: ^{84}Sr, ^{86}Sr, ^{87}Sr and ^{88}Sr, and it is an alkaline-earth element with similar geochemical behavior to Ca in natural systems (Shand et al., 2009). Variation in the Sr isotope ratios of basaltic and rhyolite rocks are reflected in the groundwater, which might give signs to hydrological pathways in the catchment and aquifer (Wiegand & Schwendenmann, 2013), given that water-rock interaction controls the ^{87}Sr/^{86}Sr isotopic ratios in groundwater (Lyons et al., 1995). ^{87}Sr is a radiogenic isotope produced from the negatron decay of radioactive ^{87}Rb (half-life of 4.88 x 10^{10} years; Faure, 1977). Although igneous minerals crystallizing from a magma may contain identical Sr isotopic ratios, the initial Rb/Sr ratios in the minerals are variable. Hence, the subsequent decay of ^{87}Rb to ^{87}Sr between the time of crystallization and today leads to differences in the present-day ^{87}Sr/^{86}Sr of different minerals (Shand et al., 2009). The Sr concentrations and ^{87}Sr/^{86}Sr are good for detecting mixing among waters of different sources because mass-dependent Sr isotope fractionation during most geochemical reactions is much smaller compared with lighter elements like H and O. Moreover, Sr is useful for characterizing the effects of water-rock interaction (Eissa et al., 2016; Eissa et al., 2012; Jørgensen et al., 2008). By water-rock interaction, minerals dissolved or leached from a rock produce a solution with ^{87}Sr/^{86}Sr isotope ratios distinctive for the weathering mineral. Therefore, the Sr isotope ratio of geothermal water can give more information about flow paths, the genesis of fluids, groundwater recharge source, and the mixing processes in geothermal systems (Wiegand et al., 2015; Lyons et al., 1995; Clark and Fritz, 1997). In general, because the felsic rocks are rich in potassium (K^+) compared to intermediate and mafic rocks, the ^{87}Sr/^{86}Sr ratios of water in contact with granites and rhyolites are high. By contrast, Sr^{2+} behaves like Ca^{2+} because these ions have similar ionic radius, charge, and electronegativity, so the abundant Ca-rich minerals (plagioclase, pyroxene) in intermediate and mafic rocks results in such rocks having lower Rb/Sr ratios and lower ^{87}Sr/^{86}Sr ratios. Hence, water-rock reactions involving intermediate and mafic rocks will result in waters with lower ^{87}Sr/^{86}Sr ratios (Lyons et al., 1995).

For the Los Azufres groundwater samples, the ^{87}Sr/^{86}Sr isotopic ratios range between 0.708913 at injection well AZ-7A to 0.703618 at production well AZ-46 (Table 4.1). Generally, deep wells located in the southern and northern parts of the investigated area have low ^{87}Sr/^{86}Sr ratios (Figure 4.10). The lowest ^{87}Sr/^{86}Sr ratios

recorded at these wells (Table 2) are mainly attributed to water-rock interaction with mafic rocks. On the other hand, the southern shallow springs in contact with felsic rocks record more radiogenic $^{87}Sr/^{86}Sr$ ratios than deep drilled wells located in both the northern and southern parts of the study area (Figure 4.10). Additionally, the most radiogenic $^{87}Sr/^{86}Sr$ ratios recorded at injection well AZ-7A is probably due to contact with more radiogenic type of rocks and facilitated by high circulation processes which give more chance for water-rock interaction with rhyolites that make up the aquifer rocks in this locality.

Figure 4.10 shows an inverse correlation between the Sr concentrations and the $^{87}Sr/^{86}Sr$ isotope ratios. In general, the deep geothermal waters are characterized by higher Sr concentrations and lower $^{87}Sr/^{86}Sr$ isotopic ratios. The lower Sr concentrations and more radiogenic $^{87}Sr/^{86}Sr$ (0.704548) are recorded at the southern spring sites (Lake - Laguna Larga and Thermal Spring / Laguna Larga Forest) they are issuing mainly from shallow felsic rhyolitic sheets that intrude the intermediate andesitic rocks (Figure 4.11) and (Figure 2.2). The northern springs have higher Sr due to andesitic rocks that rich in Ca. The $^{87}Sr/^{86}Sr$ isotopic signature of injection well AZ-7A is close to the isotopic composition of the natural spring waters located in the south, which represents the main source of feed water for the injection wells (Table 3.1).
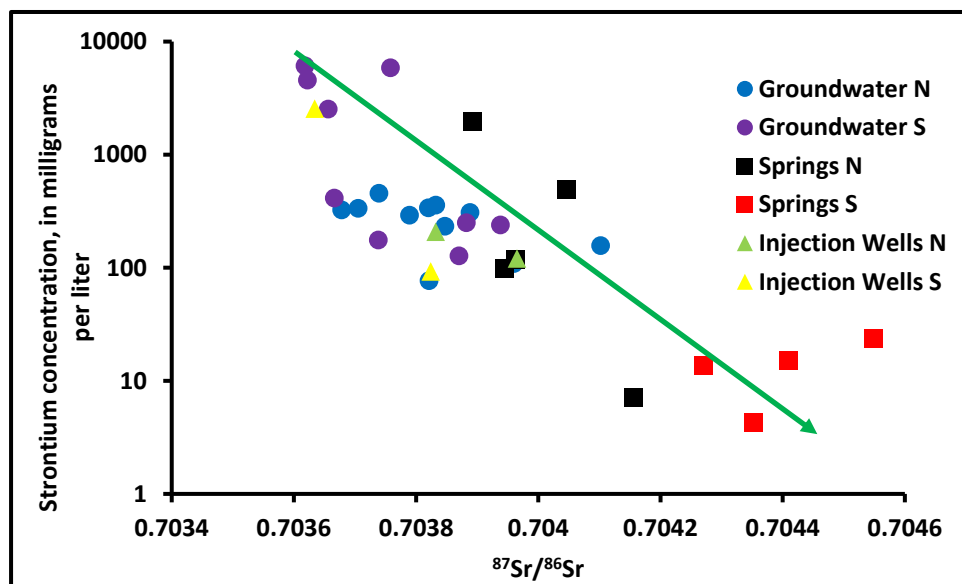
Figure 4.10 $^{87}Sr/^{86}Sr$ vs. Sr^{2+} concentration of injection wells, groundwater wells, and hot springs in the Los Azufres geothermal field.
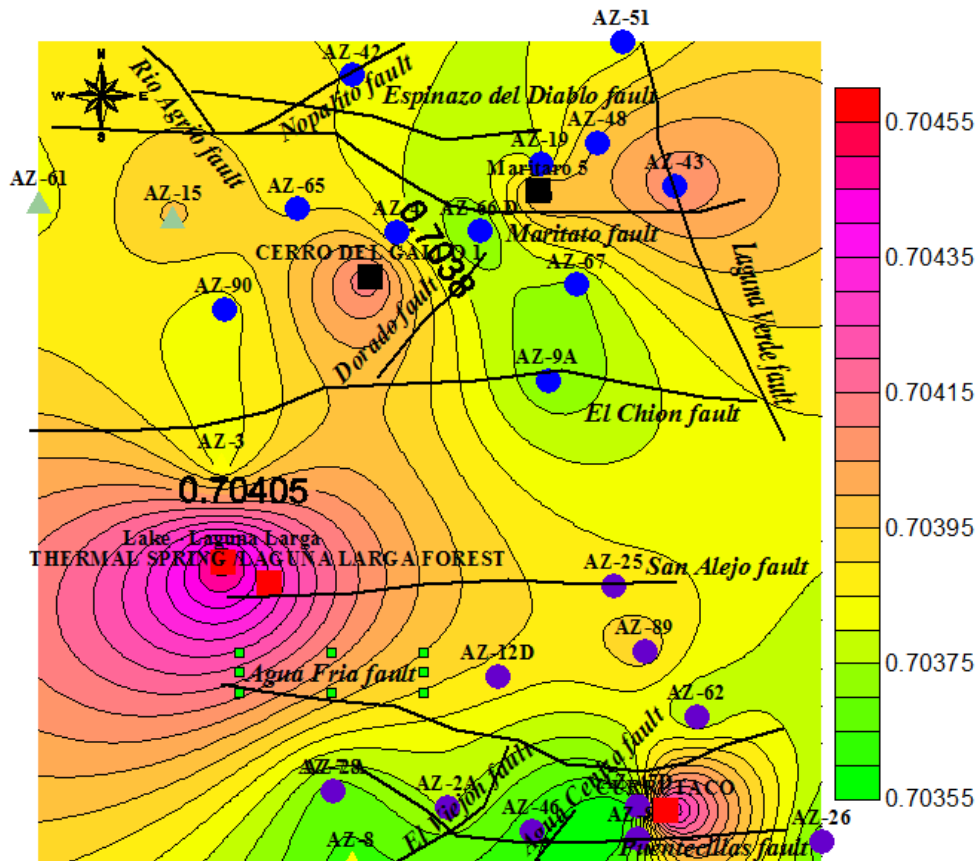
Figure 4.11 Contour map of the $^{87}Sr/^{86}Sr$ of groundwater (⬤north production wells, ⬤south production wells, △ north injection wells, and △south injection wells) and shallow water (⬛north hot springs, ⬛south hot springs) in the study area (Los Azufres geothermal field).

4.3.3 Tritium (^3H)

The radioactive hydrogen isotope tritium (^3H) is produced naturally in the atmosphere, and it has a half-life of 12.43 years. The tritium content is reported in tritium units [TU]. The ^3H concentration is used to determine the residence time of shallow water and groundwater such as spring waters and wells in fissured and fractured rocks that has aged about 100 years (Birkle et al. 2001). Because of the surface detonation of nuclear bombs, particularly between 1945 and 1963, the proportion of tritium in the atmosphere has changed over time, making it difficult to precisely calculate the residence time of the water. In this study, tritium was analyzed to identify the input of fresh meteoric water in the system.

The tritium content in the groundwater collected from the study area ranges from <0.8 TU in production wells to 4 TU at one of the springs (Lake - Laguna Larga) (Table 4.1). The shallow water springs located in the southern part of the study area

39

have the highest recorded tritium concentrations, with a mean value of 2.17 TU (Figure 4.12, 4.13). The spring samples located in the northern part of the study area showed mildly elevated tritium concentrations, with a mean value of 0.98 TU (Figure 4.12). The presence of tritium in shallow springs are mainly attributed to replenishment by precipitation, which acts as the main source of aquifer recharge that infiltrates through the fracture system in the igneous rocks.

The tritium content in groundwater of all the production and injection wells are less than 0.8 TU, with the exception of two deep injection wells located in the south and north parts of the study area (sites AZ-15 and AZ-7A) and two production wells located in the north (sites AZ-9A and AZ-67). The tritium concentration in deep injection well sites AZ-15 and AZ-7A were 0.9 TU and 1.1 TU, respectively. The presence of tritium in these two deep injection wells are mainly attributed to mixing of the reinjected water with fresh meteoric water, or exchange with the tritium in the atmosphere during its presence at the surface and before it is re-injected in the deep underground. Additionally, the presence of moderate tritium contents in the deep production wells AZ-67 (0.8 TU) and AZ-9A (1.15 TU) can be also due to the impact of the El Chion fault, which crosses these wells and facilitates the infiltration and circulation of meteoric recharge water deeper into the aquifer (Figure 4.13).

The vertical hydraulic conductivity (or vertical permeability) value of the Los Azufres aquifer matrix has been estimated to be 2.1×10^{-6} m/s (Birkle et al., 2001), which is equivalent to 66 m/year. The aquifer thickness in the study area ranges between 918 m and 2693 m at wells AZ-46 and AZ-48, respectively. Therefore, the estimated travel time for meteoric recharge water will range from 13 to 40 years, assuming a vertical path from the surface to the deep saturated zone in the aquifer. Based on the low tritium concentration in deep groundwater of the production wells in Los Azufres and the half-life of tritium (12.43 years), which is less than the estimated travel time for meteoric recharge water from the surface to the deep reservoirs, the concentration of tritium in groundwater in the study area should be low as observed.

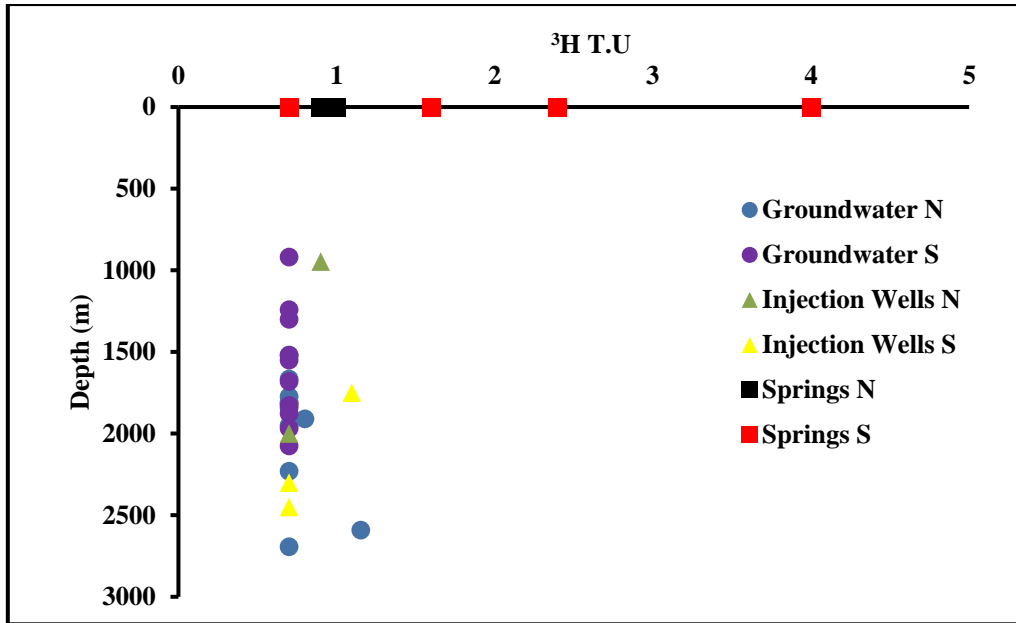**Figure 4.12 ^{3}H vs. depth of injection wells, groundwater wells, and hot springs in the Los Azufres geothermal field.**
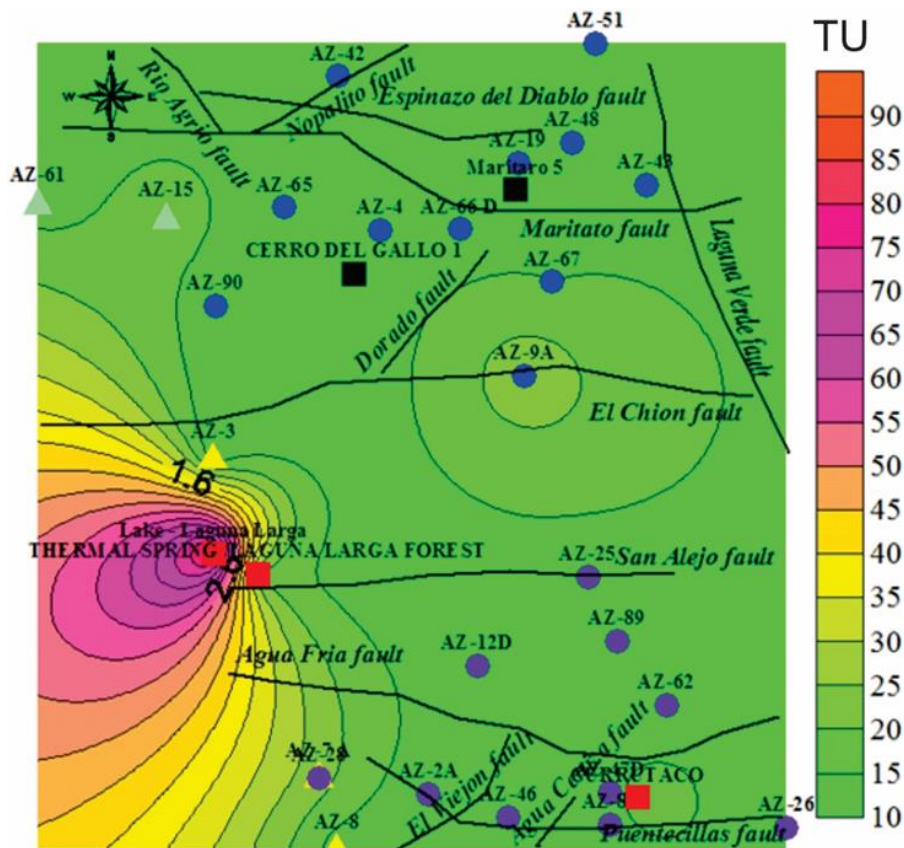

Figure 4.13 Contour map of ^{3}H (TU) of groundwater (◯north production wells, ◯south production wells, △ north injection wells, and △south injection wells) and shallow water (■north hot springs, ■south hot springs) in the study area (Los Azufres geothermal field).

4.3.4 Chlorine ($\delta^{37}Cl$) and Bromine ($\delta^{81}Br$)

Chlorine is a halogen that belongs to group 17 of the periodic table, and it is a strong tracer for fluid pathways and sources in the Earth's environment. Chlorine exists in the Earth's rocks and waters as the chloride anion (Stefánsson & Barnes, 2016). Moreover, the chlorine stable isotope compositions of rock from the crust and upper mantle, subduction zones, and ore deposits have been used to trace fluid sources (Barnes et al., 2008, 2009; Selverstone and Sharp, 2011, 2013; Chiaradia et al., 2014). It has also been used to study volcanic degassing and fluid–rock interactions; these processes are influenced by pH, salinity, and temperature (Rizzo et al., 2013; Cullen et al., 2015). Bromine also belongs to the halogen group, which also includes iodine, chlorine, bromine and fluorine. Bromide concentrations in freshwater and seawater are about 0.5 mg/l and 65 mg/l, respectively (Al-Mutaz, 2000). Chlorine and bromine isotopes have been used to investigate groundwater mixing as well as to determine recharge sources and the origin of salts dissolved in groundwater (Eissa, 2012; Eissa et al., 2015, 2016).

The chlorine ($\delta^{37}Cl$) isotope composition of groundwater in the study area ranges between 1.1‰ in injection well site AZ-61 and -1.1‰ in spring site Cerro Del Gallo 1. There is no correlation between $\delta^{37}Cl$ and well depth, and also there is no correlation between $\delta^{37}Cl$ and Cl^- concentration (Figure 4.15). Although the Cl^- concentrations in the southern production wells are typically higher than those in the northern production wells, but there $\delta^{37}Cl$ have s similar range. The north and south production wells and north injection wells in the study area have $\delta^{37}Cl$ between 0.78‰ (site AZ-67) and 0.20‰ (site AZ-43) (Figure 4.14). Unlike the southern injection wells that have $\delta^{37}Cl$ values like the production wells, the injection wells (AZ-15, AZ-61) in the northern part of the study area showed isotopic values that are higher (1.0 and 1.1‰, respectively) than those of the production wells. This suggests that the waters that re-inject in the northern part of the study area are affected by a process that changes its isotopic values to more enriched values.

The range of bromine isotope compositions ($\delta^{81}Br$) in the study area is from 0.65‰ in the north production well AZ-43 to -0.41‰ in north production well AZ-67. Figure 4.16 shows that there is some kind of a correlation between the $\delta^{81}Br$ and well depth in both parts of the study area, however, some anomalies are present. Generally

deeper wells are associated with more depleted $\delta^{81}Br$ values. Similarly, some correlation can be observed between the $\delta^{81}Br$ and bromide concentrations (figure 4.17), where, more enriched $\delta^{81}Br$ are observed with higher concentrations of Bromide. Generally, the northern part of the study area is characterized with a larger range of $\delta^{81}Br$ compared to the southern part.

Figure 4.18, shows some reverse correlation between $\delta^{37}Cl$ and $\delta^{81}Br$, especially in the northern part of the study area. The $\delta^{37}Cl$ values are between +0.1‰ and +1.2‰, and the $\delta^{81}Br$ values are between -0.4‰ and +1.2‰.
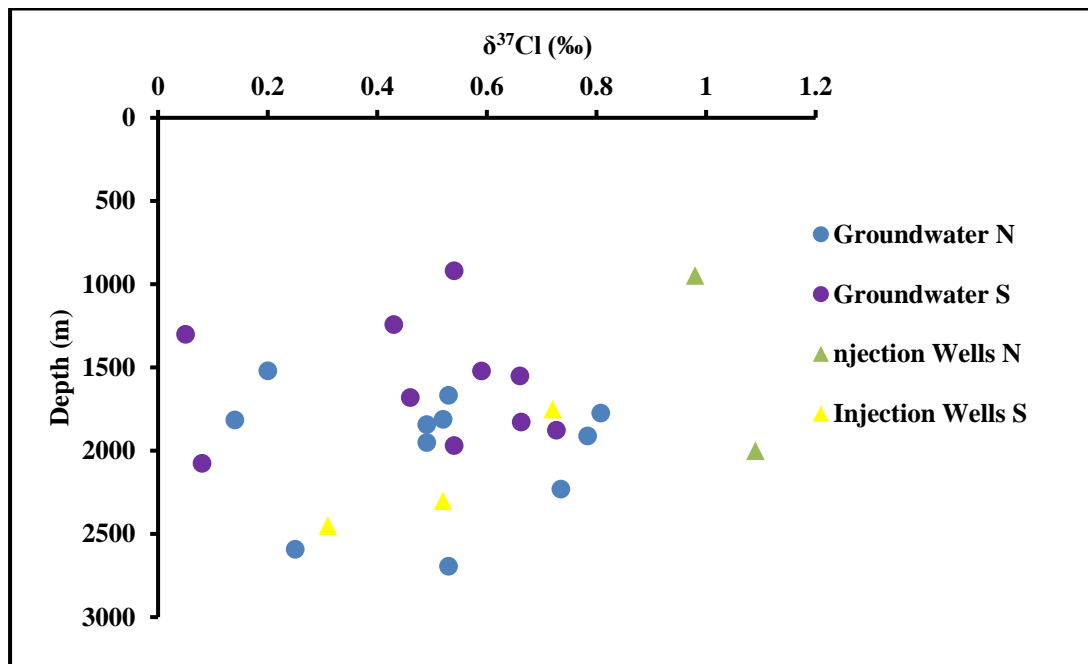
Figure 4.14 $\delta^{37}Cl$ vs. depth of injection wells, groundwater wells, and hot springs in the Los Azufres geothermal field.
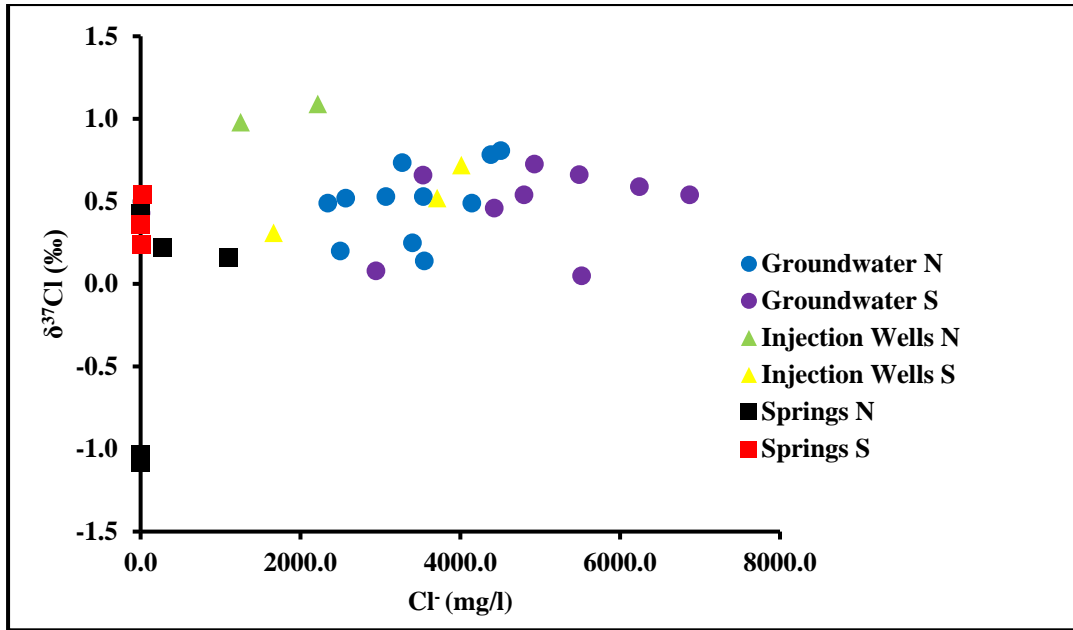
Figure 4.15 δ^{37}Cl vs. Cl$^-$ of injection wells, groundwater wells, and hot springs in the Los Azufres geothermal field.
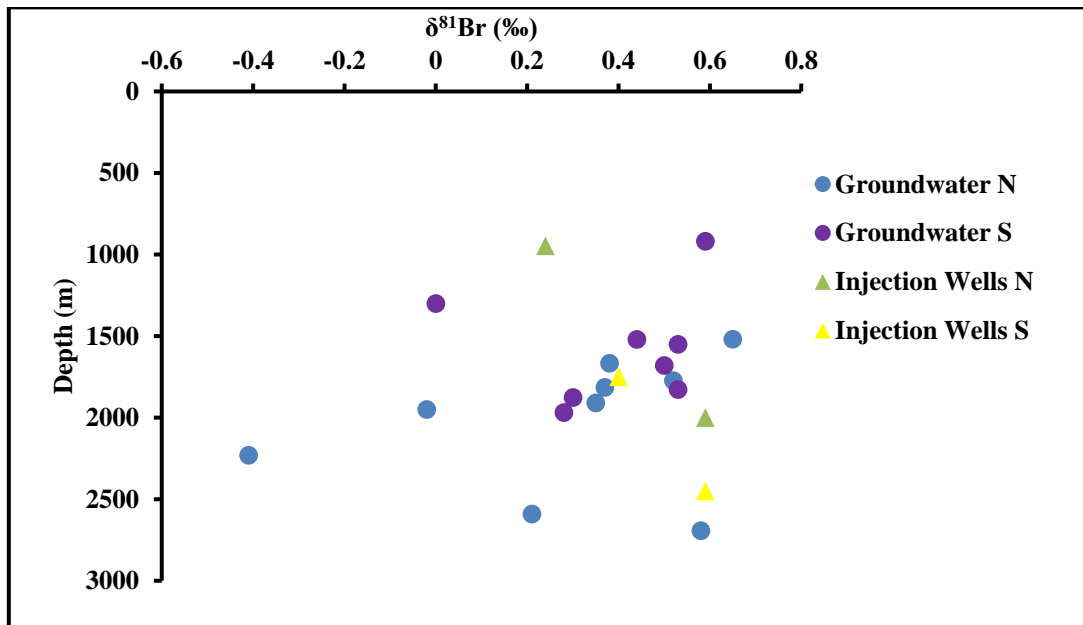
Figure 4.16 δ^{81}Br vs. depth of injection wells, groundwater wells, and hot springs in the Los Azufres geothermal field.
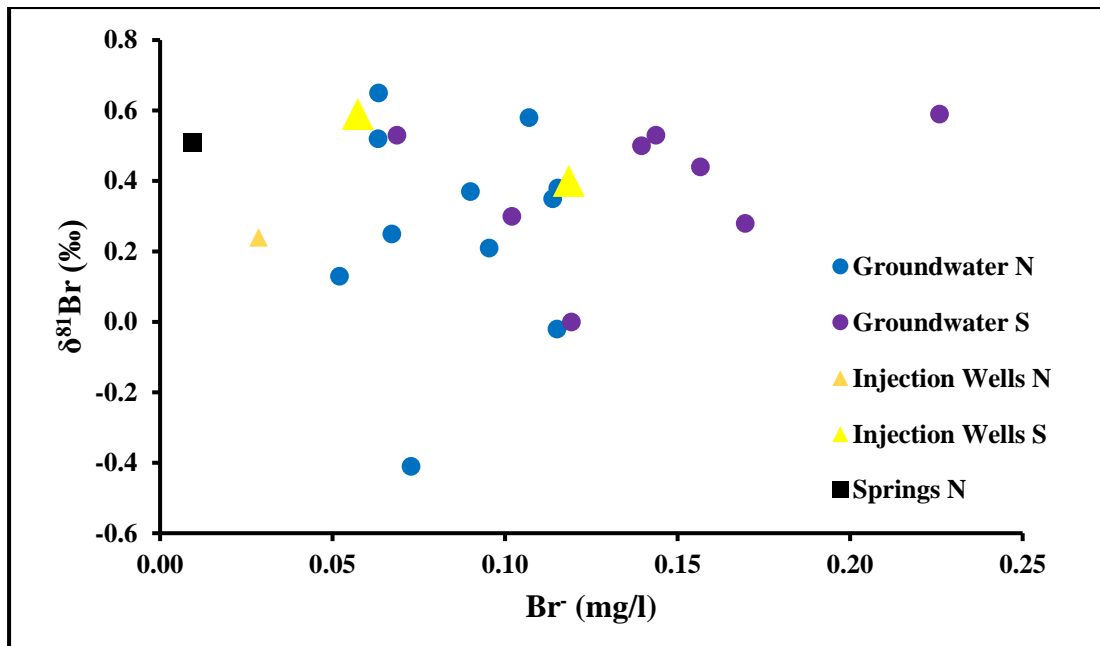
Figure 4.17 δ^{81}Br vs. Br of injection wells, groundwater wells, and hot springs in the Los Azufres geothermal field.
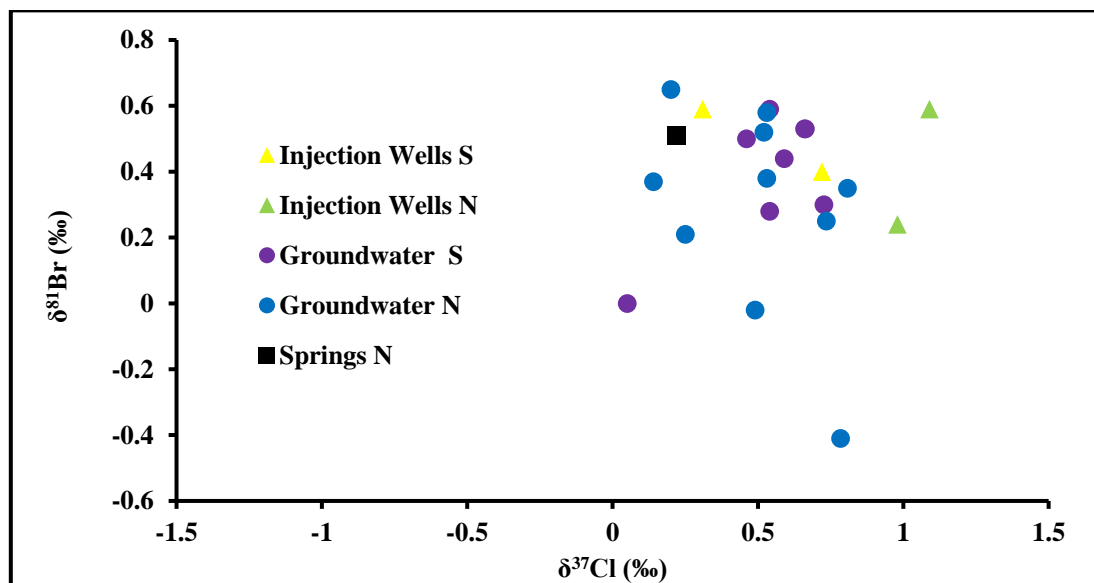
Figure 4.18 δ^{37}Cl vs. δ^{81}Br of injection wells, groundwater wells, and hot springs in the Los Azufres geothermal field.

4.4. Synthesis

In general, deep production wells in the study area seem to have the same chemical composition (Na^+ - Cl^- type waters) due to water-rock interaction with the andesites that formed the main reservoir rock. This observation is in agreement with the previous study in this area (Verma et al., 1989). In general, the samples collected from the deep production wells show pH values close to neutral. However, hot springs

in area are typically more. Data from production wells in the study area, show that the concentrations of chloride, sodium, and calcium dissolved in the deep water, have been increasing since 1984 (Tello & Suárez, 2000). In this study the chloride concentration is increased since 1987 especially in southern production wells (AZ-46, AZ-47D, AZ-2A, AZ-83, and AZ-26). Likewise, the same wells have high concentrations of (K^+, Ca^{++}, Na^+) and more enriched isotopic values ($\delta^{18}O$, δ^2H). These high concentrations of chemical elements and enriched water isotopic values suggests higher boiling processes in the southern zone compared to those in the northern zone in the study area.

The $\delta^{18}O$ and δ^2H results from the current study was compared with those obtained from previous studies (Nieva et al., 1983,1987; P.Brik et al., 2001; Pinti et al., 2013). The $\delta^{18}O$ and δ^2H values in this study are more positive than the previous results, which suggest an evolution of the isotopic signatures due to the production and re-injection processes that are probably enhancing the circulation process. The high chloride and salinity of the collected samples suggest that the water-rock interaction and isotopic exchange with the aquifer rocks is very active (Figure 4.8).The isotope compositions of the hot springs in the study area were important, as they indicate direct communication between the surface and the reservoir.

The southern shallow springs record more radiogenic Sr isotope ratios than deep drilled wells located in both the northern and southern portions of the study area as well as the northern springs of the study area (Figure 4.9). The southern springs are located mainly in a shallow felsic rhyolitic, so they have high $^{87}Sr/^{86}Sr$ ratios and low Sr concentrations (Figure 4.9). By contrast, the production wells, injection wells, and most northern springs have low $^{87}Sr/^{86}Sr$ ratios and high Sr concentrations due to water-rock interaction with andesite and basalts. The water-rock interaction thus controls the $^{87}Sr/^{86}Sr$ isotopic ratios and Sr concentrations in groundwater. The ground water from the south part of the study area (AZ-46, AZ-47D, AZ-2A, AZ-83, and AZ-26) has generally higher Sr concentrations and lower $^{87}Sr/^{86}Sr$ ratios, thus reflecting a greater extent of water-rock interaction due to higher temperatures. This is agreeing with the $\delta^{18}O$ and δ^2H isotopes and major cation/anion chemistry (K^+, Ca^{++}, Na^+) results, so, the same southern production wells have high concentrations.

According to Birkle et al. (2001), the concentrations of tritium range between 0 and 0.4 ± 0.3 TU in Los Azufres field for the geothermal liquids and gases, and this indicates that the infiltration of meteoric water into underground water reservoirs in the study area has occurred during the past 30 years. This means that the recharge is very slow in the study area, therefore, the surface water takes a long time to reach the deep reservoirs. The comparison between the current study and the Birkle et al. (2001) study showed very little change in the tritium which means that the recharge of the meteoric water is very slow.

In general, the $\delta^{37}Cl$ and the $\delta^{81}Br$ showed some reverse correlation, however the correlation could be linked to geographic distribution or any other common characteristics. There was some correlation observed between $\delta^{81}Br$ and well depth, but not between $\delta^{37}Cl$ and well depth. In general, the southern production wells show more homogenies values with smaller isotopic ranges compared to the northern production wells. The reservoir in the study area is of convective type with high temperatures fluids and the water-rock interaction induct a high temperature. Reinjection wells affects mostly wells closer to injection zones in S-W and N-W area. Reinjection water processing is useful for the energy production and longevity of this geothermal field. The south part has high water rock interaction, so drilling more wells will increase the output power.

Chapter 5 : Conclusions

5.1 Conclusion

The second most important field of geothermal energy in the northern part of Mexico is Los Azufres. Moreover, the reservoir rocks in the study area consist of igneous rocks which are rhyolite, basalt, tuff, and andesite (Figure 2.2), and these igneous rocks affect the extent of the water and rock interaction processes as well as the isotopes signature and chemical elements of the water in the study area.

Samples collected from the Los Azures geothermal field were chemically and isotopically characterized. The two parts of the Los Azufres geothermal field (north and south regions) were examined. Deep production wells from both regions seem to have the same chemical composition (Na^+ - Cl^- type waters). Water-rock interaction is obvious, especially in the production zone of the reservoir, but it is higher in the southern part of the study area then northern part, reflecting higher input of the magmatic sources and heat in the southern area. That showed at southern production wells sites (AZ-46, AZ-47D, AZ-2A, AZ-83, and AZ-26) in (K^+, Ca^{++}, Na^+, Cl^-), ($\delta^{18}O$, δ^2H), and ($^{87}Sr/^{86}Sr$). Isotopically, the southern part seems to show more confined isotopic values compared to the northern part that shows more scattered results.

The main source of the water in the study area is meteoric, and it turn into andesitic water due to water-rock interaction with the andesite rocks that formed the reservoirs. The results also showed a large impact of the andesitic water in the study area. This is clear in ($\delta^{18}O$, δ^2H), and the water type piper trilinear results.

The effect of the reinjection wells is very obvious in the western parts of the study area where most of the injection wells are located. However, the effect of the reinjection is still limited to the area surrounding the injection wells for example, temperature contour map.

The isotopic results suggest influence of meteoric water recharge into the system. The igneous rocks in the study area have many faults that allow infiltration of meteoric water into deep underground reservoirs. Moreover, that influence the isotope signatures of water in the study area, and it is clear in ($\delta^{37}Cl$, $\delta^{81}Br$) results.

The presence of water-rock interaction is also obvious in the study area especially in the production zone of the reservoir. The circulation and the water-rock interaction are higher in the southern part than the northern part of the study area, so that reflect higher input of the magmatic sources and temperature in the south part of the study area.

The results of this study were compared with the previous results in the study area. The comparison showed a change in the results over the year . The $\delta^{18}O$ and $\delta^{2}H$ previous results show that the results enrichment over the time this duo to high temperature and water rock interaction over the time. Also, the ^{3}H increased lite bait over 13years from 0.4 TU to less than 0.8 TU.

5.2. Future Work and Recommendations

There are still three important fields of geothermal energy in Mexico (Los Humeros, Las Tres Vírgenes, and Cerro Prieto) that need to be investigated. The current study is part of a major project that includes the investigation of all major geothermal fields in Mexico.

References

Al-Mutaz (2000) Water Desalination in the Arabian Gulf Region, in Water Management Purification and ConservationManagement in Arid Climates, 245-265. M.F.A. Goosen and W.H. Shayya eds., Technomic Publ.

Anguita, F., Verma, S. P., Márquez, A., Vasconcelos-F, M., López, I., & Laurrieta, A. (2001). Circular features in the Trans-Mexican Volcanic Belt. Journal of volcanology and geothermal research, 107(4), 265-274.

Appelo, C. A., & Postma, D. (1993). *Geochemistry, groundwater and pollution*. Rotterdam: A.A. Balkema.

Arellano, V. M., Torres, M. A., & Barragán, R. M. (2005). Thermodynamic evolution of the Los Azufres, Mexico, geothermal reservoir from 1982 to 2002. Geothermics, 34(5), 592-616.

Arellano, V. M., Torres, M. A., Barragán, R. M., & Sandoval, F. (2004). Respuesta a la explotación (1982-2003) del yacimiento geotérmico de Los Azufres, Mich.(México). Parte I: Zona Norte. Geotermia, 10.

Ármannsson, H., & Fridriksson, T. (2009). Application of geochemical methods in geothermal exploration. *Short Course on Surface Exploration for Geothermal Resources*.

Arnold, M., & Partida, E. G. (1987). Le système hydrothermal actuel de Los Humeros (Mexique): Etat du système SO−− 4—SH2 à 300° C, origine du soufre et phénomènes d'oxydation associés à l'ébullition du fluide ascendant. Mineralium Deposita, 22(2), 90-98.

Arriaga, M. C. S. (2002). Emission of some rare gases at the Los Azufres, Mexico, geothermal reservoir. Geofisica Internacional-Mexico-, 41(4), 467-474.

Barbier, E. (2002). Geothermal energy technology and current status: an overview. *Renewable and Sustainable Energy Reviews*, *6*(1), 3-65.

Barbier, E., Fanelli, M., & Gonfiantini, R. (1983). Isotopes in geothermal energy exploration. *Geotherm. Energy Mag.;(United States)*, *11*(9).

Barnes, J. D., Sharp, Z. D., & Fischer, T. P. (2008). Chlorine isotope variations across the Izu-Bonin-Mariana arc. Geology, 36(11), 883-886.

Barnes, J.D., Sharp, Z.D., Fischer, T.P., Hilton, D.R., Carr, M.J., 2009. Chlorine isotope variations along the Central American volcanic front and back arc. Geochem. Geophys. Geosyst.10, Q11S17.

Bertani, R. (2016). Geothermal power generation in the world 2010–2014 update report. *Geothermics*, *60*, 31-43.

Birkle, P. (2005). Compositional link between thermal fluids in Mexican deep reservoirs. In *Proc. World Geothermal Congress* (pp. 24-29).

Birkle, P., Merkel, B., Portugal, E., & Torres-Alvarado, I. S. (2001). The origin of reservoir fluids in the geothermal field of Los Azufres, Mexico—isotopical and hydrological indications. Applied geochemistry, 16(14), 1595-1610.

Cathelineau, M. C., Oliver, R., & Nieva, D. (1987). Geochemistry of volcanic series of the Los Azufres geothermal field (Mexico). Geofísica Internacional, 26(2).

Chiaradia, M., Barnes, J. D., & Cadet-Voisin, S. (2014). Chlorine stable isotope variations across the Quaternary volcanic arc of Ecuador. Earth and Planetary Science Letters, 396, 22-33.

Clark, I., Fritz, P., 1997. Environmental Isotopes in Hydrogeology, Lewis Publishers, New York.

Cole, D. R., & Ohmoto, H. (1986). Kinetics of isotopic exchange at elevated temperatures and pressures. *Reviews in Mineralogy and Geochemistry*,*16*(1), 41-90.

Craig, H. (1963). The isotopic geochemistry of water and carbon in geothermal areas.Nuclear Geology on Geothermal Areas—Spoleto, 17-53.

Cullen, J. T., Barnes, J. D., Hurwitz, S., & Leeman, W. P. (2015). Tracing chlorine sources of thermal and mineral springs along and across the Cascade Range using halogen concentrations and chlorine isotope compositions. Earth and Planetary Science Letters, 426, 225-234.

Dansgaard W (1964) Stable isotopes in precipitation. Tellus 16:436–468.

Daum, C ans M. Savina. "Geology Basics: Rocks and Minerals, Plate Tectonics, Climate History, Surface Water and Groundwater." Agriculture and the American Midwest: Literature and the Environment. 30 Nov. 2000. Carleton U. 6 Sept.2005 <http://www.acad.carleton.edu/curricular/GEOL/classes/geo120/geology_basic

Dobson, P. F., & Mahood, G. A. (1985). Volcanic stratigraphy of the Los Azufres geothermal area, Mexico. Journal of Volcanology and Geothermal Research, 25(3), 273-287.

Eissa, M. (2012). Groundwater Resource Sustainability in Wadi Watir Watershed, Sinai, Egypt. University of Nevada, Reno.

Eissa, M. A., Thomas, J. M., Pohll, G., Shouakar-Stash, O., Hershey, R. L., & Dawoud, M. (2016). Groundwater recharge and salinization in the arid coastal plain aquifer of the Wadi Watir delta, Sinai, Egypt. Applied Geochemistry, 71, 48-62.

Eissa, M.A., Parker, B., Shouakar-Stash, O., Hosni, M.H., EL Shiekh, A., 2015. Electrical resistivity tomography, geochemistry and isotope tracers for salt water intrusion characterization along the Northwestern coast, Egypt. Geological Society of America Abstracts with Programs. 47(7), 486.

Flores-Armenta, M. (2012). Geothermal Activity and Development in Mexico – Keeping the Production Going. "Short Course on Geothermal Development and Geothermal Wells", UNU-GTP and LaGeo, in Santa Tecla, El Salvador, March 11-17, 2012.

Fridleifsson, I. B. (2000). Geothermal Energy for the Benefit of the People World-wide. Web site www. geothermic. de.

Gat, J. R., Mazor, E., & Tzur, Y. (1969). The stable isotope composition of mineral waters in the Jordan Rift Valley, Israel. Journal of Hydrology, 7(3), 334-352.

Geothermal Energy Association. (2014). 2013 Geothermal Power: International Market Overview. *Sep-2013*.

Giggenbach, W. F. (1992). Isotopic shifts in waters from geothermal and volcanic systems along convergent plate boundaries and their origin. Earth and planetary science letters, 113(4), 495-510.

Gioietta Kuo. (2012). Geothermal Energy. World Future Review, P5-7.

González-Partida, E., Carrillo-Chávez, A., Levresse, G., Tello-Hinojosa, E., Venegas-Salgado, S., Ramirez-Silva, G., ... & Camprubi, A. (2005). Hydro-geochemical and isotopic fluid evolution of the Los Azufres geothermal field, Central Mexico. *Applied Geochemistry*, *20*(1), 23-39.

Gutierrez, A., & Aumento, F. (1982). The Los Azufres, Michoacan, Mexico, geothermal field. Journal of hydrology, 56(1-2), 137147149-145162.

Hannan& Scientific & all. (2012), Trace contaminant analysis in brine using a Thermo Scientific iCAP 6000 Series Duo ICP-OES, UK Eivind Rosland, Research Scientist, Borregaard, Sarpsborg, Norway

Hem, J. D. (1985). Study and interpretation of the chemical characteristics of natural water (Vol. 2254). Department of the Interior, US Geological Survey.

Hiriart, G. (2003). A new 100-MW Geothermal power project starts operations Near Morelia, Michoacán in Central Mexico. Geothermal Resources Council Bulletin, 208-211.

Jørgensen, N. O., Andersen, M. S., & Engesgaard, P. (2008). Investigation of a dynamic seawater intrusion event using strontium isotopes ($87\,Sr/86\,Sr$). Journal of Hydrology, 348(3), 257-269.

Kagel, A. (2006). A handbook on the externalities, employment, and economics of geothermal energy. *Washington, DC: Retrieved September*, *29*, 2011.

Kern, W. (1990). The evolution of silicon wafer cleaning technology. Journal of the Electrochemical Society, 137(6), 1887-1892.

Liu, Y., Kaiser, E., & Avdalovic, N. (1999). Determination of trace-level anions in high-purity water samples by ion chromatography with an automated on-line eluent generation system. Microchemical journal, 62(1), 164-173.

Lyons, W. B., Tyler, S. W., Gaudette, H. E., & Long, D. T. (1995). The use of strontium isotopes in determining groundwater mixing and brine fingering in a playa spring zone, Lake Tyrrell, Australia. Journal of Hydrology, 167(1), 225-239.

Manoj, K., Ghosh, S., & Padhy, P. K. (2013). Characterization and classification of hydrochemistry using multivariate graphical and hydrostatical techniques. Research Journal of Chemical Sciences

Marini, L. (2000). Geochemical techniques for the exploration and exploitation of geothermal energy. *Italy: University of Genua*.

Martínez, A. I. M. (2013). Case history of Los Azufres- Conceptual Modelling in a Mexican Geothermal Field. Revista Mexicana De Geoenergia· ISSN 0186 5897, 3.

Matthess, G.E.O.R.G. (1982). *The Properties of Groundwater* . New York: John Wiley & Sons.

Mazor, E., & Truesdell, A. H. (1984). Dynamics of a geothermal field traced by noble gases: Cerro Prieto, Mexico. Geothermics, 13(1), 91-102.

Nicholson, K. (1993). Geothermal Fluids Chemistry & Exploration Technique Springer Verlag. *Inc. Berlin*.

Nieva, D., & Nieva, R. (1987). Developments in geothermal energy in Mexico—part twelve. A cationic geothermometer for prospecting of geothermal resources. Heat recovery systems and CHP, 7(3), 243-258.

Nieva, D., Quijano, L., Garfias, A., Barragán, R. M., & Laredo, F. (1983). Heterogeneity of the liquid phase, and vapor separation in Los Azufres (Mexico) geothermal reservoir (No. SGP-TR-74-32). Instituto de Investigaciones Electricas, Cuernavaca, Morelos 62000, Mexico.; Subgerencia de Estudios; Coordinadora Ejecutiva de Los Azufres, Gerencia de Proyectos Geotermoelectricos, Comision Federal de Electricidad.

Pang, Z. (1992). Theoretical calibration of chemical geothermometers, in Water Rock Interaction, Rotterdam, pp 1463-1466.

Pang, Z. H., & Wang, J. Y. (1990). Oxygen and hydrogen isotope study on Zhangzhou basin hydrothermal system, southeast of China. *Geothermal Resources Council. Transactions*, *14*, 945-951.

Pickler, C., Pinti, D. L., Ghaleb, B., Garduno, V. H., & Tremblay, A. (2012). Radium depletion and 210 Pb/226 Ra disequilibrium of Marítaro hydrothermal deposits, Los Azufres geothermal field, Mexico. Geochemical Journal, 46(6), 493-504.

Pinti, D. L., & Marty, B. (1998). The origin of helium in deep sedimentary aquifers and the problem of dating very old groundwaters. Geological Society, London, Special Publications, 144(1), 53-68.

Pinti, D. L., Castro, M. C., Shouakar-Stash, O., Tremblay, A., Garduño, V. H., Hall, C. M., ... & Ghaleb, B. (2013). Evolution of the geothermal fluids at Los Azufres, Mexico, as traced by noble gas isotopes, δ^{18}O, δD, δ^{13}C and ^{87}Sr/^{86}Sr. *Journal of Volcanology and Geothermal Research*, *249*, 1-11

Polyak, B. G., Prasolov, E. M., Čermák, V., & Verkhovskiy, A. B. (1985). Isotopic composition of noble gases in geothermal fluids of the Krušné Hory Mts., Czechoslovakia, and the nature of the local geothermal anomaly. Geochimica et Cosmochimica Acta, 49(3), 695-699.

Pradhan, B., & Pirasteh, S. (2011). Hydro-Chemical analysis of the ground water of the basaltic catchments: Upper Bhatsai Region, Maharastra. Open Hydrology Journal, 5, 51-57.

Prasolov, E. M., Polyak, B. G., Kononov, V. I., Verkhovskii, A. B., Kamenskii, I. L., & Prol, R. M. (1999). Inert gases in the geothermal fluids of Mexico. Geochemistry international, 37(2), 128-144.

Rizzo, A. L., Caracausi, A., Liotta, M., Paonita, A., Barnes, J. D., Corsaro, R. A., & Martelli, M. (2013). Chlorine isotope composition of volcanic gases and rocks at Mount Etna (Italy) and inferences on the local mantle source. Earth and Planetary Science Letters, 371, 134-142.

Selverstone, J., & Sharp, Z. D. (2011). Chlorine isotope evidence for multicomponent mantle metasomatism in the Ivrea Zone. Earth and Planetary Science Letters, 310(3), 429-440.

Selverstone, J., & Sharp, Z. D. (2013). Chlorine isotope constraints on fluid-rock interactions during subduction and exhumation of the Zermatt-Saas ophiolite. Geochemistry, Geophysics, Geosystems, 14(10), 4370-4391.

Shand, P., Darbyshire, D. P. F., Love, A. J., & Edmunds, W. M. (2009). Sr isotopes in natural waters: Applications to source characterisation and water–rock interaction in contrasting landscapes. Applied Geochemistry, 24(4), 574-586.

Stefánsson, A., & Barnes, J. D. (2016). Chlorine isotope geochemistry of Icelandic thermal fluids: Implications for geothermal system behavior at divergent plate boundaries. Earth and Planetary Science Letters, 449, 69-78.

Taylor, M. A. (2007). The State of Geothermal Technology. *Part*, *1*, 29-30.

Tello, M. R., & Suárez, M. C. (2000). Geochemical evolution of the Los Azufres, Mexico, geothermal reservoir. Part I: Water and salts. In Proceedings World, Geothermal Congress (pp. 2257-2262).

Torres-Alvarado, I. S. (1996). Wasser/Gesteins-wechselwirkung im geothermischen Feld von Los Azufres, Mexiko. Mineralogische, thermochemische und isotopen geochemische Untersuchungen. Tuebinger Geowissenschaftliche Arbeiten, Reihe E, 2.

Truesdell, A. H., & Hulston, J. R. (1980). Isotopic evidence on environments of geothermal systems. In Handbook of environmental isotope geochemistry. Vol. 1.

Truesdell, A. H., Rye, R. O., Pearson, F. J., Olson, E. R., Nehring, N. L., Whelan, J. F., ... & Coplen, T. B. (1979). Preliminary isotopic studies of fluids from the Cerro Prieto geothermal field. Geothermics, 8(3-4), 223-229.

Verma, M. P., Nieva, D., Santoyo, E., Barragan, R. M., & Portugal, E. (1989). A hydrothermal model of Los Azufres geothermal system, Mexico.

Verma, S. P. (1985). On the magma chamber characteristics as inferred from surface geology and geochemistry: examples from Mexican geothermal areas. Physics of the Earth and Planetary Interiors, 41(2), 207-214.

Viggiano-Guerra, J.C., and Gutiérrez-Negrín, L.C.A. (1995). Comparison between two contrasting geothermal fields in Mexico: Los Azufres and Los Humeros. *Proceedings of the World Geothermal Congress 1995*, Volume 3, Florence, Italy, 18-31 May 1995.

Wang, J. Y., & Pang, Z. H. (1995). Application of isotope and geochemical techniques to geothermal exploration in Southeast China—A review. geochemical techniques applied to geothermal investigations, 9.

Welhan, J. A., Poreda, R., Lupton, J. E., & Craig, H. (1979). Gas chemistry and helium isotopes at Cerro Prieto. Geothermics, 8(3), 241-244. (1)Retrieved from http://www.ecofriend.com/eco-tech-new-geothermal-power-plant-could-provide-a-tenth-of-uks-electricity.html

West JEC, Inc. and JBIC, 2007: Feasibility Study of the Los Azufres III Geothermal Energy Expansion Project, Michoacán, México. Comisión Federal de Electricidad (CFE), Geothermal Project Management, 360 pp.

55

Wiegand, B. A., & Schwendenmann, L. (2013). Determination of Sr and Ca sources in small tropical catchments (La Selva, Costa Rica)–A comparison of Sr and Ca isotopes. *Journal of hydrology*, *488*, 110-117.

Wiegand, B. A., Brehme, M., Kamah, Y., & Sauter, M (2015). Distribution of Sr and Ca Isotopes in Fluids of Lahendong Geothermal Field.

Zhong-He, Pang, and Wang Ji Yang. "Application of isotope and geochemical techniques to geothermal exploration-the Zhangzhou Case." *World Geother Cong* (1995): 1037-1041.